ELSEVIER

Coordination Chemistry Reviews 146 (1995)
91–140

COORDINATION CHEMISTRY REVIEWS

2. Zirconium 1992

Sylvia M. Draper and Brendan Twamley

CONTENTS

INTRODUCTION 91
2.1 ZIRCONIUM(IV) 92
2.1.1 Complexes with hydride ligands 92
2.1.2 Complexes with coordinating carbon ligands 93
2.1.3 Complexes with silicon donor ligands 99
2.1.4 Complexes with nitrogen donor ligands 99
2.1.5 Complexes with phosphorus donor ligands 105
2.1.6 Complexes with oxygen donor ligands 110
2.1.7 Complexes with sulfur donor ligands 114
2.1.8 Complexes with halide ligands 116
2.1.9 Heterometallic complexes 116
2.2 ZIRCONIUM(III) 122
2.2.1 Complexes with hydride ligands 122
2.2.2 Complexes with coordinating carbon ligands 124
2.2.3 Complexes with nitrogen donor ligands 124
2.2.4 Complexes with phosphorus donor ligands 126
2.2.5 Complexes with halide ligands 126
2.3 ZIRCONIUM(II) 127
2.3.1 Complexes with nitrogen donor ligands 127
2.3.2 Complexes with phosphorus ligands 128
2.4 ZIRCONIUM(0) 128
2.5 CATALYTIC USES OF ZIRCONIUM COMPLEXES 129
2.6 ZIRCONIUM INTERCALATION COMPOUNDS 135
2.7 ZIRCONIUM CLUSTERS 136
REFERENCES 137

INTRODUCTION

This chapter surveys the literature published on the coordination chemistry of zirconium in 1992. It is comprehensive for the main journals, which were searched manually, and *via* Current Contents, the Cambridge Crystallographic Data Base and STN International searches. Those references from more obscure sources were reviewed using *Chemical Abstracts* (vol. 117, 118). Incorporated into this review are three sections which briefly cover catalytic uses of zirconium complexes, zirconium intercalation compounds and zirconium clusters.

SSDI 0010-8545(95)01196-X

2.1 ZIRCONIUM(IV)

2.1.1 Complexes with hydride ligands.

Prolonged treatment of $Zr(BH_4)_4$ or $Hf(BH_4)_4$ with 4.5 equivalents of PMe_3 (5 hours) gives the first trinuclear group 4 polyhydrides $[M_3H_6(BH_4)_6(PMe_3)_4]$ (M = Zr, Hf) (Figure 1). The ^1H, ^{31}P and ^{11}B NMR spectroscopic data are consistent with the X-ray crystal structure of the Zr complex which contains a noncyclic $M(\mu\text{-}H)_3M(\mu\text{-}H)_3M$ backbone. Several of the $\eta^3\text{-}BH_4$ groups are asymmetrically bonded resulting in the lengthening of one Zr-H bond (2.26(4)Å) compared to the other two (~2.10(4)Å). In each case the long Zr-H bond to the BH_4^- group is approximately *trans* to a Zr(2)-H-Zr(3) bridging hydride. Multinuclear NMR spectra indicate that in solution three dynamic processes are occurring firstly to interconvert the $\eta^2\text{-}BH_4^-$ and $\eta^3\text{-}BH_4^-$ groups on Zr(1), secondly to interconvert the three tridentate BH_4^- groups on Zr(3) and thirdly to produce two hydride environments rather than the six required by the solid-state structure. Addition of 1,2-bis(dimethylphosphino)ethane to $Zr_2H_3(BH_4)_5(PMe_3)_2$ results in phosphine exchange and loss of one BH_3 unit to yield $Zr_2H_4(BH_4)_4(dmpe)_2$. The NMR spectroscopic and X-ray crystallographic data show that three hydrides bridge the Zr...Zr axis and that the remaining hydride, one $\eta^2\text{-}BH_4$ group and the two dmpe ligands coordinate to only one zirconium centre. Variable temperature NMR spectroscopic data indicate that the terminal and bridging hydrides exchange with an activation barrier of 12.6 ± 0.1 kcal mol^{-1} [1].

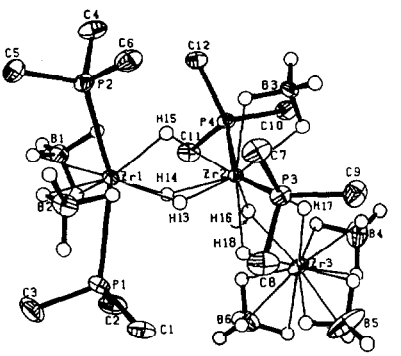

Figure 1. Molecular structure of $Zr_3H_6(BH_4)_6(PMe_3)_4$ showing the 35% probability surfaces. The hydrogen atoms are represented by arbitrarily-sized spheres. Reproduced with permission from ref. [1].

The cation $[(C_5H_4Me)_2Zr(H)(thf)]^+$ rearranges slowly (weeks, ambient temperature, or 48h, 60°C) with opening of the thf ligand to yield $[(C_5H_4Me)_2Zr(O^nBu)(thf)]^+$. Exchange of the H^- and $^nBuO^-$ ligands between the $ZrCp'_2$ centres results indirectly in H/D exchange at the β–Cp'-H sites of this complex (equ (1)). The hydride undergoes H/D exchange as shown in equ. (1) but there is no H/D exchange at the $\alpha\text{-}C_5H_4Me$-H or $C_5H_4Me\text{-}CH_3$ sites. It is proposed that H/D exchange at the $\beta\text{–}C_5H_4Me$-H site involves an intermediate formed by D_2 addition across a $Zr\text{-}C_5H_4Me$ bond (equ (2)) [2].

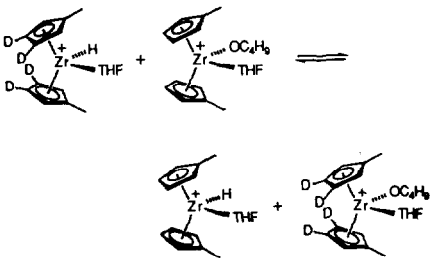

(1)

Reproduced with permission from ref. [2].

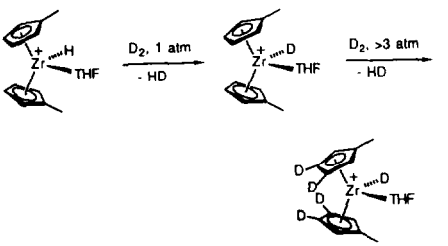

(2)

Reproduced with permission from ref. [2].

The reaction of permethylzirconocene dihydride with 1,4-pentadiene and 1,5 hexadiene yields $Cp^*_2(H)ZrCH_2(CH_2)_nCH_2Zr(H)Cp^*_2$ (n = 3,4) and $[Cp^*_2\overline{ZrCH_2(CH_2)_nCH(CH_3)}]$ (n = 2, 3). These products were obtained in solution in benzene-d^6, and decompose on standing [3].

2.1.2 *Complexes with coordinating carbon ligands.*

The bis(trimethylsilyl) substituted thiophenes (Figure 2) are synthesised from the zirconocene mediated cyclisation of 1,7-bis(trimethylsilyl)-1,6-heptadiyne and 1,8-bis(trimethylsilyl)-1,7-octadiyne followed by reaction with SCl_2. In contrast, when a heteroatom, A, is present in the diyne, air-stable zirconium complexes are obtained that react with SCl_2 to give starting materials, or protonolysis of the Zr-C bond to produce 1,3-dienes. Further studies to examine the stabilising affects of the heteroatom A and the substituents R (Figure 3), are underway [4].

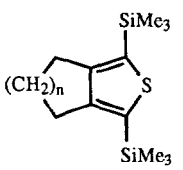

1. n = 1
2. n = 2

Figure 2

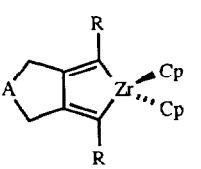

A = O, R = $SiMe_3$
A = $PhCH_2N$, R = $SiMe_3$
A = $PhSO_2NH$, R = $SiMe_3$
A = $PhCH_2N$, R = $Si(^iPr)_3$
A = $PhCH_2N$, R = $Si(Ph_2{}^tBu)_3$

Figure 3

In general, chiral strapped metallocenes e.g. the ethylenebis(1-indenyl) complex of Zr(IV), are prepared in an equal mixture of racemic and meso forms, despite the fact that the meso isomer would be expected to be less stable on steric grounds. The only effective method of racemic-meso interconversion is by irradiation to the photostationary phase. The ligand (*S,S*)-2,3-butylene-1,1'-bis(indene) (Figure 4) was prepared from diindenylmagnesium and the dimesylate of (*R,R*)-2,3-butanediol. Reaction of the dilithium salt of this ligand with $ZrCl_4$.2thf in thf produced [Zr(*S,S*)-chiracene)Cl_2] isomers (~18%). The kinetic ratio of these being *R,S*:*R,R*:*S,S* = 19:1:1. The meso isomer (*R,S*) was readily crystallised from this mixture and the solid state structure was obtained (Figure 5). Photolysis of the mixture (450 W Hg lamp, 240 nm cut off) gave a photostationary state consistiing of *R,R*:*S,S* = 5.2:1. These results differ from the tin(IV) analogue [5].

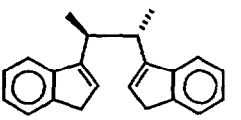

Figure 4

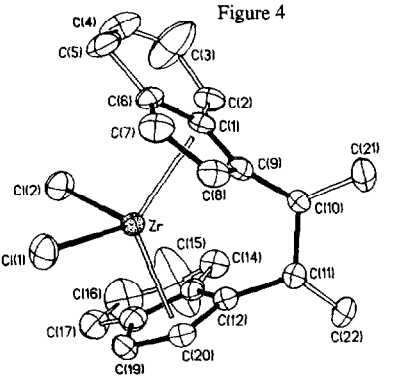

Figure 5. Molecular structure and labelling scheme for (*R,S*)-[Zr((*S,S*)-chiracene)Cl_2] drawn with 40% probability ellipsoids. Reproduced with permission from ref. [5].

Indenylsodium reacts with chiral *trans*-1,2-dimesyl cyclohexane to give *trans*-1,2-diindenyl cyclohexane, a ligand precursor for the preparation of a mixture of diastereomeric cyclohexyl-[*trans*-1,2-bis(1-indenyl)]zirconium(IV)dichlorides (Scheme 1). These catalyse the polymerisation of propene with high stereoselectivity even above 50°C in contrast to the catalytic behaviour of ethylenebis(1-indenyl)zirconium(IV)dichloride [6].

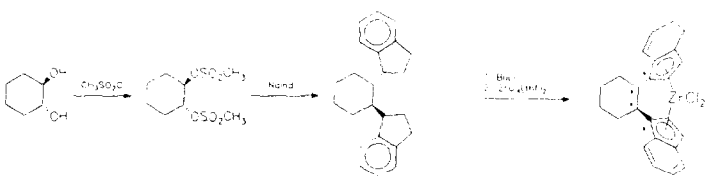

Reproduced with permission from ref. [6].

Scheme 1

The compound $Cp''_2Zr\{CH(SiMe_3)_2\}Cl$ reacts with one equivalent of $AlCl_3$ to form the Lewis adduct $Cp''_2Zr\{CH(SiMe_3)_2\}Cl.AlCl_3$ (Cp''_2 = *rac*-$C_2H_4(indenyl)_2$, $(C_5H_5)_2$). In contrast $Cp''_2Zr\{CH_2SiMe_3\}Cl$ reacts with $AlCl_3$ to undergo rapid alkyl-chloride exchange to form $Cp''_2ZrCl_2.(Me_3SiCH_2)AlCl_2$ (Cp''_2 = *rac*-$C_2H_4(indenyl)_2$, $(C_5Me_5)_2$). $Cp''_2Zr\{CH(SiMe_3)_2\}Cl$ reacts with two equivalents of $AlCl_3$ to give the novel Si-C bond activated products $[Cp''_2Zr\{CH(SiMe_2Cl)(SiMe_3)\}][Al_2Cl_nMe_{7-n}]$ (Cp''_2 = *rac*-$C_2H_4(indenyl)_2$, $(C_5H_5)_2$) (equ (3)). The formation of the latter may involve an agostic coordination of a Si-Me bond to zirconium and subsequent chloride nucleophilic attack at silicon. This reaction is reversible as shown by the formation of *rac*-$C_2H_4(indenyl)_2Zr\{CH(SiMe_3)_2\}Cl$, on the reaction of $[Cp'_2Zr\{CH(SiMe_2Cl)(SiMe_3)\}][Al_2Cl_nMe_{7-n}]$ with a two fold excess of $AlCl_3$. The structure of the latter (where n = 0.5) was obtained by X-ray crystallography. The anion formulation is the result of a 1:1 mixture of $[AlCl_7]^-$ and $[Al_2Cl_6Me]^-$ in the crystalline state. The crystal structure is suggestive of partial Si-C multiple bond character (Zr-Si 3.132(1) Å) [7].

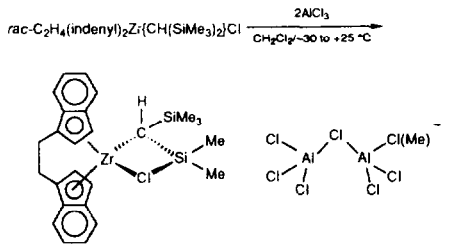

Reproduced with permission from ref. [7]. (3)

The complex $(C_5Me_5)(C_5H_5)ZrCl_2$ reacts with 2 equivalents of $LiCH_2PPh_2.TMEDA$ to give the dialkyl derivative $[(C_5Me_5)(C_5H_5)Zr(CH_2PPh_2)_2]$. When 1 equivalent of $LiCH_2PPh_2$ is used a mixture of the dialkyl complex and the starting material are produced. Characterisation of the products was obtained by ^1H, ^{13}C, and $^{31}P\{^1H\}$ NMR spectroscopy and elemental analysis. The ^1H NMR spectrum showed that the methylene protons exhibit diastereotopic behaviour with resonances that appear as *pseudo* doublets at δ 0.22 and δ 0.81 (J_{HH} = 11 Hz) [8].

The reaction of the dilithium salt of 2-cyclopentadienyl-2-fluorenylpropane in pentane with $ZrCl_4$ gives the complex $(\eta^5\text{–}C_5H_4CMe_2\text{-}\eta^5\text{–}C_{13}H_8)ZrCl_2$, which has been characterised in the solid state by X-ray diffraction methods. The complex is an active catalyst precursor for the homogeneous polymerisation of α–alkenes and when activated by methylalumoxane, promotes the polymerisation of propylene to give highly syndiotactic polypropylene. The mechanism of this catalysed process appears to be enantiomorphic-site stereochemical control [9].

The reaction of excess ^tBuCCH with a 1:1 mixture of $[Cp_2ZrMe_2]$ and $[PhMe_2NH][BPh'_4]$ generates an unstable salt $[Cp_2ZrMe(NMe_2Ph)][BPh'_4]$ (Ph' = 4-C_6H_4F). When this mixture is warmed to 25°C and the reaction monitored by ^1H and ^{13}C NMR spectroscopy, the presence of a new electron deficient dizirconocene cation is detected (equ (4)). The latter has been isolated and its solid state structure obtained. The presence of an agostic C(1)-H(1a)-Zr(1) interaction is confirmed by the crystal structure data (Zr(1)-C(1) = 2.616(14)Å, Zr(1)-H(1a) = 2.27(15)Å). Similar reactions

with less crowded alkynes RCCH (R = ^{i}Pr, ^{n}Pr, 4-tolyl) yield 1,1-dimetalloalkenes, in which there is an unprecedented alkenylidene unit bridging the two d° metal centres (equ (5)). The ^{13}C NMR spectroscopic resonances for the Cα and Cβ nuclei are indicative of this type of interaction (δ 304.9, δ 159.1 respectively) [10].

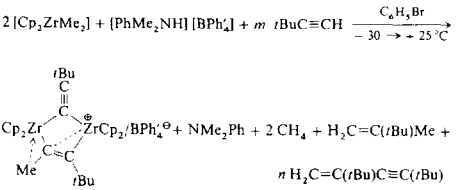

Reproduced with permission from ref. [10]. (4)

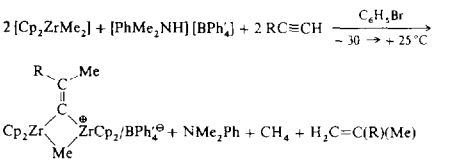

Reproduced with permission from ref. [10]. (5)

In order to examine the relationship between agostic interactions at the metal-carbon bond in early transition metal organometallic complexes and their catalytic polymerisation of unsaturated hydrocarbons, a theoretical study using EH-MO calculations and relating $J_{(CH)}$ values obtained from a series of ethylene coordinated complexes has been undertaken. Experimental work on some new zirconocene and hafnocene systems includes a crystal structure of Cp_2Hf(s-*cis*-1,4-diphenyl-1,3-butadiene) [11].

The reaction of symmetrically substituted biphenyl bridged bis(cyclopentadienyls) with $ZrCl_4(thf)_2$ gives *ansa*-metallocenes to the preclusion of the formation of diastereomers (equ (6)). The bridged complex was extracted in 3% yield from hot hexane and characterised by ^{1}H NMR spectroscopy, which revealed that the β-CH_3 groups are inequivalent. The structure was confirmed using X-ray diffraction methods [12].

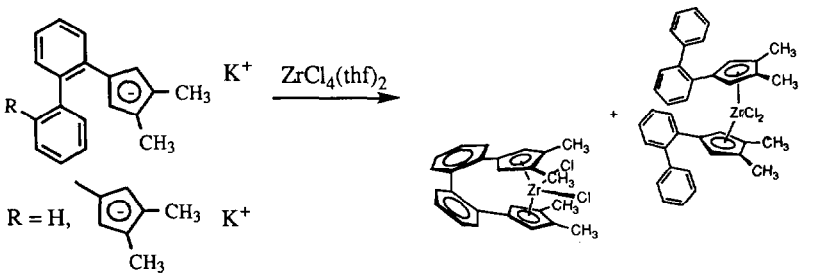

(6)

Reproduced with permission from ref. [12].

The synthesis and properties of *ansa*-zirconocene dichlorides with two different cyclopentadienyl units have been reported using epoxystyrene as a building block as shown (Scheme 2). A low temperature X-ray structure investigation of *rac*-[1-(η^5–cyclopentadienyl)-1-phenyl-2-(tetraphenyl-η^5–cyclopentadienyl)ethane] zirconium confirmed the chiral arrangement of the four phenyl substituents of the C_5Ph_4 unit. A ^1H NMR spectroscopic study showed that the phenyl groups rotate rapidly at room temperature generating equivalent *ortho* proton positions on each C_5-Ph_4 substituent. The more hindered phenyl rings freeze out between -40 and -60°C into a conformation where the *ortho* protons are inequivalent, one pointing inwards and one outward from the zirconocene sandwich [13].

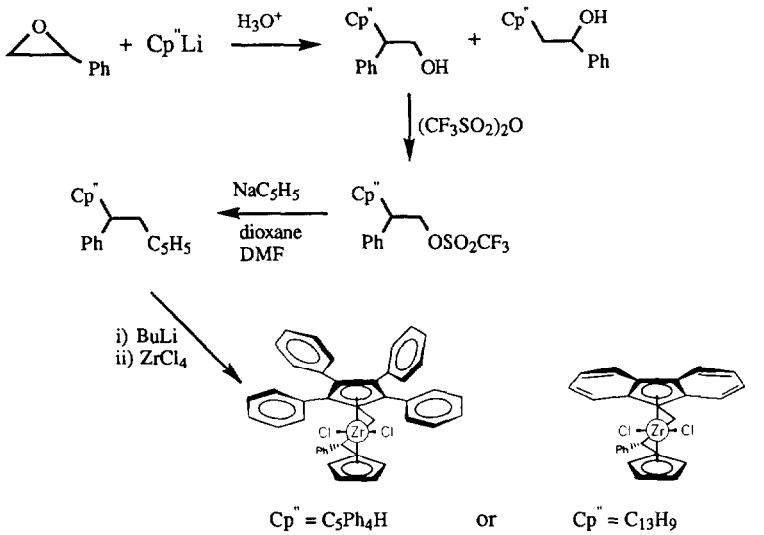

Cp" = C_5Ph_4H or Cp" = $C_{13}H_9$

Reproduced with permission from ref. [13]. *Scheme 2*

The reactions of dibasic tridentate hydrazones, monobasic benzothiazolines, 1,2-di(o-aminophenylthio)ethane and a dibasic hexadentate Schiff base with Cp_2ZrCl_2 have been studied and the products have been analysed from elemental analysis, molar conductances, molecular weights, and IR, UV-VIS and ^1H NMR spectroscopic data [14].

The labile nature of the coordinated anion in the Lewis base-free complex $(C_5Me_5)_2ZrMe\{B(4\text{-}C_6H_4F)_4\}$ results in a highly electrophilic metal centre which is reactive with respect to the addition of 1,2 or 1,3-dienes. Addition of 1,3-butadiene results in an unusual C-H activation product $[(C_5Me_5)Zr\{\eta^5{:}\eta^3\text{–}C_5Me_4(CH_2CH_2CHCHCH_2)\}]^+[B(4\text{-}C_6H_4F)_4]^-$ which contains a tetramethylcyclopentadienyl-$(CH_2)_2$-allyl ligand. The η^3–coordination of the allyl fragment has been confirmed by assignment of all the resonances in 2D COSY ^1H NMR spectroscopic experiments. The formation of this complex proceeds *via* an unstable η^3–allyl, formulated as $[(C_5Me_5)_2Zr\{\eta^3\text{–}(Me)\text{-}CHCHCH(Me)\}]^+$ on the basis of ^1H NMR spectroscopic data. The analogous reaction in bromobenzene with 1,2-propadiene forms $[Cp'_2Zr\{\eta^3\text{–}CH_2C(Me)CH_2\}]^+$ (Cp' = C_5Me_5, $(Me_3C)C_5H_4$) *via* insertion of the diene into the Zr-Me bond (Scheme 3) [15].

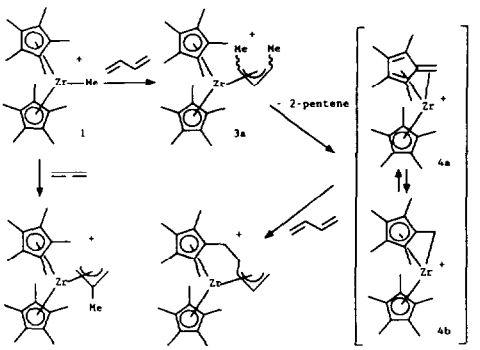

Scheme 3. Formation of cationic complexes (the anion $[B(4\text{-}C_6H_4F)_4]^-$ has been omitted). Reproduced with permission from ref. [15].

The reaction of *in situ* generated $[Zr(C_5Me_5)Me\{B(4\text{-}C_6H_4F)_4\}]$ with an excess of RCCH (R = ^{t}Bu, ^{n}Pr) results in the formation of the unprecedented complexes $[Zr(C_5Me_5)_2\{CH{=}C(R)CCR\}]^+$, which can be purified by crystallisation. These products have been characterised by ^1H, ^{13}C, and ^{19}F NMR spectroscopy and elemental analysis. Analogous products result from the equivalent reactions with MeCCH, PhCCH or $(4\text{-}C_6H_4Me)CCH$, but these are powdered or oily solids. The reaction of $[Zr(C_5Me_5)Me\{B(4\text{-}C_6H_4F)_4\}]$ with three equivalents of Me_3SiCCH and a further excess of alkyne gives a novel complex containing a 1,4,6-trisubstituted-hexa-1,3-diene-5-yn-1-yl ligand formed by 2,1-alkyne insertion into the Zr-C bond of $[Zr(C_5Me_5)_2\{CH{=}C(SiMe_3)CC(SiMe_3)\}]^+$. Preliminary studies show that $[Zr(C_5Me_5)Me\{B(4\text{-}C_6H_4F)_4\}]$ catalyses the rapid regioselective oligomerisation of RCCH to 2,4-disubstituted-but-1-en-3-ynes (R = ^{t}Bu, ^{n}Pr, Me, Ph, $4\text{-}C_6H_4Me$) and 1,4,6-trisubstituted-hexa-1,3-dien-5-ynes (R = ^{n}Pr, Me). Proton NMR spectroscopic monitoring of these reactions has led to the formulation of a catalytic cycle, showing that the reaction of $[Zr(C_5Me_5)_2\{CH{=}C(R)CCR\}]^+$ with an excess of alkyne occurs *via* σ-bond metathesis and the release of $H_2C{=}C(R)CCR$ or alkyne insertion [16].

The novel $-C(CH_3)_2$-bridged molecule $(CH_3)_2C(C_5H_4)_2Zr(CH_3)_2$ was synthesised and spectroscopically characterised. The solid state structure shows considerable distortion of the ideal tetrahedral geometry about the metal centre [17].

The electronic structure of $Cp_2\overline{Zr(CH_2SiMe_2CH_2)}$ has been investigated by a combination of SCF Hartree-Fock-Slater discrete vibrational Xα calculations and HeI, HeII UV-photoelectron spectroscopy. The complex is best described electronically as a heterodinuclear molecule containing bridging $\mu\text{-}CH_2$ groups. The formation of the four-membered ring involves stabilising interactions between higher-lying empty orbitals of the bridging $\mu\text{-}CH_2$ groups and appropiate metal orbitals of the metallocene fragment. Population of the internal metallacycle molecular orbitals causes a redistribution of electron densities and partially restores the d^2 metal configuration [18].

2.1.3 Complexes with silicon donor ligands.

The electronic structure of complexes of the type $R''_nM{=}SiRR'$, (M = Zr, Hf) have been investigated using *ab initio* wave functions including the effects of electron correlation. Several conclusions have been made: firstly that the inclusion of electron correlation is necessary to describe the MSi-π bond, secondly, that the GVB overlap and MSi force constants increase on the electron withdrawing nature of the ligands (e.g. R = Cl) and thirdly, that the MSi force constants vary, with Nb > Zr and Ta > Hf. Analysis of the molecular and electronic structural data using the MC/LMO/CI approach implies that stronger MSi double bonds occur when the MSi π-bond has more back-bonding character [19].

2.1.4 Complexes with nitrogen donor ligands.

The reaction of Cp_2ZrCl_2 with lithium amides or the thermolysis of Cp_2ZrMe_2 in the presence of suitable primary amines produces zirconium bisamides $Cp_2Zr(NHR)_2$ or alkylamides $Cp_2Zr(NHR)(R')$. The former catalyse the hydroamination of alkynes and allene. Kinetic studies of the catalytic and stoichiometric additions of 2,6-dimethylaniline to diphenylacetylene in the presence of $Cp_2Zr(NH(2,6\text{-}C_6H_3(CH_3)_2)_2$ at 95°C are consistent with a reversible rate determining α-elimination of amine and the generation of a transient imido complex $Cp_2Zr{=}NR$ which reacts competitively with either alkyne or amine. The latter results in the formation of cycloaddition products, azametallacyclobutenes (Scheme 4). These are rapidly protonated by $ArNH_2$ at the zirconium-carbon bond to give enamide amides which subsequently undergo α-elimination to regenerate $Cp_2Zr{=}NR$. The connectivity of $Cp_2Zr{=}NR$ was confirmed by a single crystal X-ray study. The ability of the bisamide starting materials to undergo the steps postulated in the catalytic cycle is dependent on the size of the zirconium bound amide ZrNHR e.g. thermolysis of $Cp_2Zr(NH(SiMe_2{}^tBu))_2$ with PhCCPh at 140°C results in no reaction after 6 days [20].

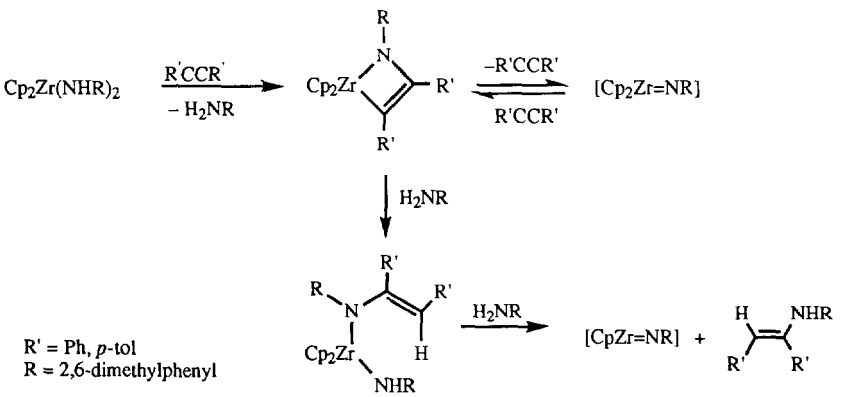

Scheme 4

The complex (η^4–butadiene)zirconocene reacts with one equivalent of benzonitrile to give a five-membered azazirconacyclopentene derivative which reacts further with benzonitrile to form a chiral nine-membered metallacycle as shown in Scheme 5. This Zr-NH containing complex is the

kinetically controlled product and converts slowly into the (imido)zirconium tautomer after heating at 60°C for 1 week. This complex was characterised by X-ray diffraction and crystallises with benzene as a solvent molecule at a centre of inversion. On hydrolysis, a single isomer of 1,6-diphenyl-1,3,5-hexatriene-1,6-diamine is obtained. The Gibbs activation energy of the enantiomerisation of $[Cp_2ZrN{=}C(Ph)CH_2CH{=}CHCH_2C(Ph){=}N]$ was calculated from dynamic ^1H NMR spectroscopic studies to be $\Delta G^{\ddagger}(323K) = 15.5 \pm 0.3$ kcal mol^{-1}. The analogous conformational equilibration of $[Cp_2ZrN(H)C(Ph){=}CHCH{=}CHCH_2C(Ph){=}N]$ has a lower activation barrier, $\Delta G^{\ddagger}(236K) = 12.1 \pm 0.3$ kcal mol^{-1} [21].

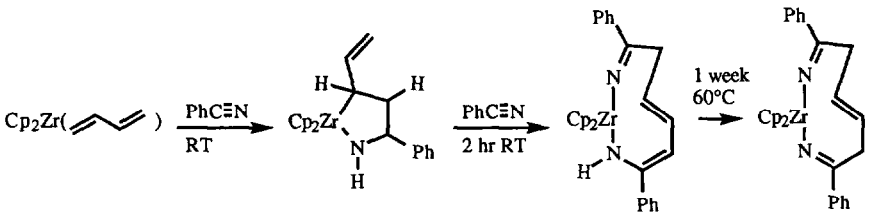

Scheme 5

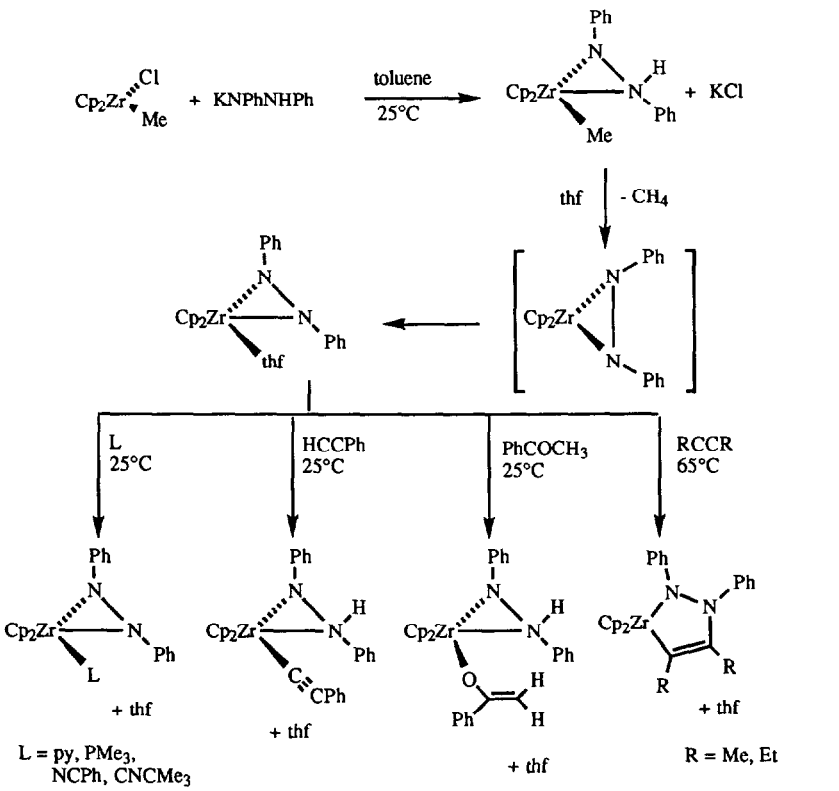

Scheme 6

The synthesis and reactivity of methyl-η^2–1,2-diphenylhydrazido(-1)zirconocene has been examined as shown (Scheme 6). All these species have been characterised using ^1H and $^{13}C\{^1H\}$ NMR spectroscopy. Notably the product zirconocene-2,3-diazametallacyclopentene $Cp_2Zr((Ph)NN(Ph)C(Me)C(Me))$ has been structurally characterised by single crystal X-ray diffraction and results from the insertion of 2-butyne into the metal-nitrogen bond of $[Cp_2Zr(N_2Ph_2)(thf)]$ [22].

The chloride $ZrCl_4$ reacts with two equivalents of $Li[N(SiHMe_2)_2]$ in diethyl ether to give $[ZrCl(\mu\text{-}Cl)\{N(SiHMe_2)_2\}_2]_2$ (Figure 6). Infrared spectroscopic data (ν(Si-H) = 1948 cm^{-1}) and a single crystal X-ray structure analysis of this compound provide evidence for an unprecedented type of β–hydrogen interaction between a hydrogen attached to a silicon atom of the bis(dimethylsilyl)amide ligand and the zirconium atom [23].

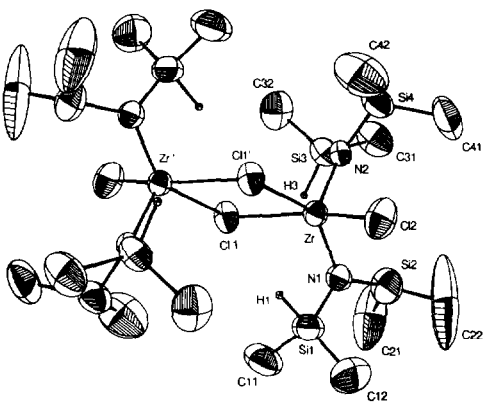

Figure 6. ORTEP drawing of $[ZrCl(\mu\text{-}Cl)\{N(SiHMe_2)_2\}_2]_2$ with thermal ellipsoids of 50% probability. Reproduced with permission from ref. [23].

Zirconium tetrachloride reacts with $LiNH^tBu$ to give $[(^tBuNH)_2ZrN^tBu]_2$ which is thermally unstable and oligomerises with the elimination of H_2N^tBu above 100°C. Similar reactions between $(\eta^5\text{–}C_5Me_5)ZrCl_3$ and LiNHR give the thermally stable products $(\eta^5\text{–}C_5Me_5)Zr(NHR)_3$ (R = ^{t}Bu, 2,4,6-$Me_3C_6H_2$, 2,6-$^i Pr_2C_6H_3$) and the dimer $[(\eta^5\text{–}C_5Me_5)Zr(NHPh)NPh]_2$. Pyridine can be used to replace one molecule of 2,6-$^i Pr_2C_6H_3NH_2$ in $[(\eta^5\text{–}C_5Me_5)Zr(NH(2,4,6\text{-}Me_3C_6H_2))_3]$ to give $[(\eta^5\text{–}C_5Me_5)Zr(NH(2,4,6\text{-}Me_3C_6H_2))N(2,4,6\text{-}Me_3C_6H_2).py]$ which has been characterised in the solid-state by X-ray crystallography [24]. The reaction of lithiated pyrrole and $ZrCl_4$ gives (2,5-$C_4{}^tBu_2RHN)ZrCl_3$ (R = H, $SiMe_3$). The π-coordination of the azacyclopentadienyl ligand is indicated from the ^{13}C NMR spectroscopic data and is observed in the solid-state structure of the Ti analogue (R = H) [25].

Ammonolysis of benzene solutions of $(^tBu_3CO)Zr(CH_2Ph)$ with one equivalent of NH_3 yields colourless crystals of a composite which consists of pseudo-octahedral $[(^tBu_3O)Zr]_6(\mu_6\text{-}N)(\mu_3\text{-}NH)_6(\mu_2\text{-}NH_2)_3$ and square pyramidal $[(^tBu_3O)Zr]_5(\mu_5\text{-}N)(\mu_3\text{-}NH)_4(\mu_2\text{-}NH_2)_4$ in which the μ_3-NH groups cap the trigonal faces and the μ_2-NH_2 units bridge the basal zirconium atoms.

The structures were confirmed by single crystal X-ray studies, ^{1}H, $^{13}C\{^{1}H\}$ and CPMAS ^{15}N NMR spectroscopy. The latter was critical in identifying the nitride (δ -62.6), imide (δ -141.1, J_{NH} = 61Hz) and amide ligands (δ -302.2, J_{NH} = 60Hz). Treatment of $(^{t}Bu_3O)Zr(CH_2Ph)$ with 1.75 equivalents of NH_3 gave pure $[(^{t}Bu_3O)Zr]_5(\mu_5\text{-}N)(\mu_3\text{-}NH)_4(\mu_2\text{-}NH_2)_4$ in 32% yield. Addition of 2.6 equivalents of NH_3 gives the dodecaamide cluster $[(^{t}Bu_3O)Zr]_5(\mu_5\text{-}N)(\mu_2\text{-}NH_2)_{12}$. The structure of this species is ambiguous but NMR spectroscopic studies indicate that the compound has a square pyramidal configuration with three sets of μ_2-NHH' groups and 7-coordinate basal zirconium atoms about the μ_5-nitride. In solution this dodecaamido nitride is prone to ammonia loss and exists in equilibrium with $[(^{t}Bu_3O)Zr]_5(\mu_5\text{-}N)(\mu_3\text{-}NH)_4(\mu_2\text{-}NH_2)_4$ and four equivalents of NH_3 [26].

An *ab initio* study of methane activation by the imido complexes $H_2M{=}NH$ (M = Ti, Zr, Hf) has been carried out. The polarity of the metal-ligand bond in the alkane complexes $H_2M(CH_3)(NH_2)$ formed initially plays an important role in facilitating subsequent C-H scission. Calculated methane activation barriers Ti>Zr>Hf are in line with calculated exothermicities. Calculated methane elimination barriers are in agreement with experimental models in terms of absolute numbers and trends as a function of the metal atom. Calculated geometries indicate a late transition state for methane elimination. The TS_s has an obtuse angle about the H atom of the C-H bond being activated (H_t) and a short MH_t distance. The latter implies a stabilising interaction supported by a positive overlap population [27].

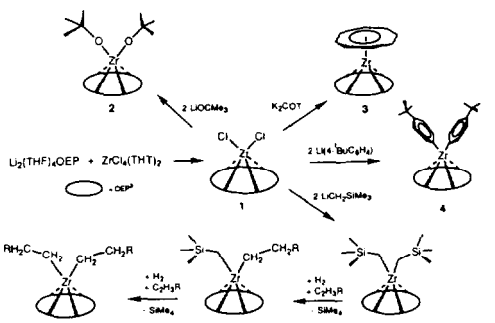

Reproduced with permission from ref. [28]

Scheme 7

The synthesis of several unprecedented metalloporphyrin derivatives from $(OEP)_2ZrCl_2$ is outlined in the Scheme 7. The *cis*-alkoxide derivative forms dark red moisture sensitive crystals in toluene/hexane and shows a high-field signal at δ -0.38 in the ^{1}H NMR spectrum for the tert-butoxide protons due to shielding by the porphyrin ligand. The formation of the *cis* isomer is indicated by the presence of diastereotopic methylenes. The molecular structure of the *cis*-dialkyl complex was confirmed by single crystal X-ray crystallography and showed that the Zr-C distances (2.285(4)Å and 2.289(4)Å) were extremely similar to those found in $Cp_2Zr(CH_2SiMe_3)_2$. Preliminary studies of this complex show it to promote the catalytic hydrogenation of propene and ethene [28].

The simple metathesis between $(OEP)ZrCl_2$ and $[nido\text{-}7,8\text{-}C_2B_9H_{11}]^{2-}$ gives 74% of the air-stable metalloporphyrin-carbaborane sandwich compound $(OEP)Zr(\eta^5\text{-}1,2\text{-}C_2B_9H_{11})$ (Figure 7)

on recrystallisation. The product has been characterised in the solid state by mass spectrometry and single crystal X-ray crystallography, and in solution by ^{1}H, $^{11}B\{^{1}H\}$, $^{13}C\{^{1}H\}$ NMR and UV spectroscopy. The solid-state structure shows that the zirconium atom lies 0.904Å out of the nitrogen plane and 2.096Å from the face of the C_2B_9 ligand. The carbaborane ligand is tilted with respect to the porphyrin ring such that the normals of the two bonding faces form an angle of 4.9°. This distortion is ascribed to crystal packing effects [29].

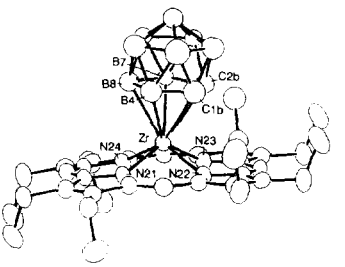

Figure 7. ORTEP view of the molecular structure of (OEP)Zr(η^5-$C_2B_9H_{11}$). Reproduced with permission from ref. [29]

The reaction of $Cp(PMe)_3RuCH{=}CHZrClCp_2$ with ^{t}BuNC produces $Cp(PMe_3)_2RuCH{=}CHC(N^{t}Bu)ZrClCp_2$ of which there are two isomeric forms. The initially formed kinetic product has the *N*-donor portion of the η^2–iminoacyl ligand on the outside of the three ligation sites of the Cp_2Zr moiety. This isomer cleanly converts to the thermodynamic "N-inside" isomer with activation parameters $\Delta H^{\ddagger} = 19.9 \pm 0.6$ kcal mol^{-1}, $\Delta S^{\ddagger} = -3.4 \pm 2.2$ cal K^{-1} mol^{-1}, $\Delta G^{\ddagger}(298K) = 20.9$ kcal mol^{-1}. Spectroscopic and crystallographic data for the latter indicate a zwitter-ionic resonance form (Scheme 8). Similarly a zwitterion contribution was observed in the related η^2–iminoacyl complexes $Cp(PMe_3)_2RuCH{=}CHC(NMe)ZrClCp_2$ and $Cp(PMe_3)_2RuCH{=}C(CH_3)C(NMe)ZrClCp_2$ but was not observed in the methylated dimetalloalkene $Cp(PMe_3)_2RuCH{=}C(CH_3)C(N^{t}Bu)ZrClCp_2$ due to steric inhibition of resonance [30].

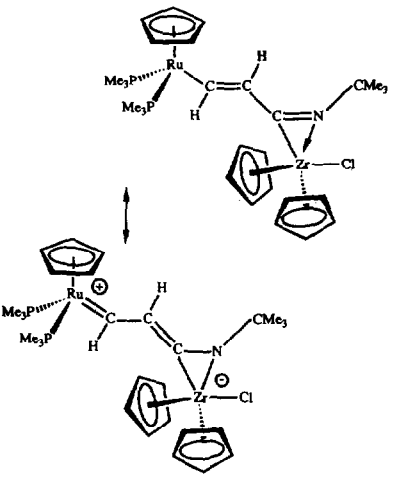

Reproduced with permission from ref. [30].

Scheme 8

Eight coordinate complexes of ethylenedioxydiethylene dinitrilotetraacetate (egta4$^-$) [Zr(egta)] and [Hf(egta)] have been prepared in aqueous solution from the reaction of $M(OH)_4$ (M = Hf, Zr) and H_4egta. The two compounds were isostructural in the solid state with distorted square antiprismatic coordination geometry. The ^{1}H NMR spectroscopic data for [Zr(egta)] show that all the methylene groups in this system are inequivalent [31]. Compounds of general formula $MZrL.3H_2O$ (M = K, guandinium, H_5L = diethylenetriaminepentaaceticacid) were prepared and their structures determined from X-ray diffraction data. The potassium salts crystallise in a triclinic space group whereas the guandinium salts crystallise in a monoclinic space group [32].

The compound $[Cp_2Zr(CH_3)(thf)][BPh_4]$ reacts with 2,6-diethylpyridine to afford a chelated secondary zirconocene-alkyl complex $[Cp_2Zr(\eta^2$-C,N-CH{Me}{6-ethylpyrid-2-yl})$]^+$. Treatment of this species with $(PhCH_2)(Et)_3N^+Cl^-$ gives [Cp$_2$Zr(CHMe){6-ethylpyrid-2-yl}][Cl] which has been structurally characterised using single crystal X-ray diffraction (Figure 8). Complexes with general formula $[Cp_2Zr(CHMe)\{6\text{-ethylpyrid-2-yl}\}(L)]^+$ are produced from the reaction of [Cp$_2$Zr(CHMe){6-ethylpyrid-2-yl}][Cl] with CO, CH_3CN, ^{t}BuCN (L) whose spectroscopic data compare well with [Cp$_2$Zr(CHMe){6-ethylpyrid-2-yl}][Cl]. $[Cp_2Zr(CHMe)\{6\text{-ethylpyrid-2-yl}\}(CO)]^+$ is a rare example of a d^0 M(alkyl)CO-adduct and was characterised from low temperature solution NMR and IR spectroscopy (the ^{13}C NMR spectrum at -40°C exhibits a resonance at δ206.1 for the coordinated CO). As a CO_2Cl_2 yellow solution, this compound decomposes to form a transient cationic zirconocene-acyl intermediate *via* CO insertion into the Zr-C bond which then undergoes a 1,2-H shift to afford a mixture of isomeric/oligomeric zirconocene-enolates. The formation of such species was confirmed by the reaction of this mixture with $(PhCH_2)(Et)_3N^+Cl^-$ which yielded [Cp$_2$Zr(OCH=C{Me}{6-ethylpyrid-2-yl}][Cl] as a mixture of E/Z isomers and by hydrolysis [33].

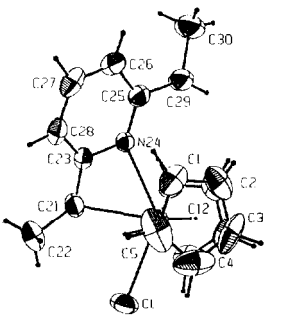

Figure 8. Crystal structure of [Cp$_2$Zr(CHMe){6-ethylpyrid-2-yl}][Cl]. Reproduced by permission from ref. [33].

The synthesis of (dimethylamino)alkylzirconocene complexes has been acheived by reacting Cp_2ZrCl_2 or Cp$_2$Zr(Me)Cl with a suitable group I amine (Scheme 9). Reaction of Cp$_2$Zr(Me)CH(Ph)NMe$_2$ with acidic reagents (CF_3CO_2H, $CpMo(CO)_3H$, [^{n}Bu$_3$NH][BPh$_4$]) resulted in cleavage of the methyl ligand and the -O_2CCF_3, -(μ-OC)Mo(CO)$_2$Cp complexes or the solvated cation respectively. Proton NMR spectroscopic data on all these complexes showed that the methyl (Me_2N) groups were inequivalent at low temperature, indicating that in each case the CH(R)NMe$_2$ ligands were coordinated to the metal in an η^2 fashion. [Cp$_2$Zr{(μ-

OC)Mo(CO)$_2$Cp}CH(Ph)NMe$_2$] was found to undergo *N*-methyl exchange in $CDCl_3$ solutions. Simulation of its temperature dependent ^1H NMR spectra gave a $\Delta H^{\ddagger}$ value of 17.1±0.8 kcal mol^{-1}, the Zr-N interaction energy being ~8 kcal mol^{-1}. [Cp$_2$Zr(Cl)CH$_2$N(CH$_3$)$_2$] does not react with excess LiCH$_2$N(CH$_3$)$_2$, LiPh, MeI, $CO_{(g)}$ 1 atm or Na(Hg) but a small amount of its methyl derivative is obtained on treatment with $LiCH_3$ [34].

$$Cp_2ZrClR + PhCH(K)NMe_2 \xrightarrow[thf]{-78°C} Cp_2Zr(R)CH(Ph)NMe_2 + KCl$$

$$Cp'CpZrCl_2 + LiCH_2NMe_2 \xrightarrow[thf]{-78°C} CpCp'Zr(Cl)CH_2N(CH_3)_2 + LiCl$$

Cp' = Cp, $C_5H_4C(CH_3)_2Ph$

Scheme 9

2.1.5 *Complexes with phosphorus donor ligands.*

The reaction of Cp*$_2$ZrCl$_2$ with two equivalents of LiPH(C$_6$H$_2$Me$_3$) in benzene at 25°C yields 90% of a diphosphido species initially, but on standing for several days, fractional crystallisation of the phosphametallocycle Cp*$_2$Zr(CH$_2$C$_6$H$_2$Me$_2$PH) and a second zirconium derivative Cp*$_2$ZrP(C$_6$H$_2$Me$_3$)$_2$ occurs [35]. These three species appear to exist in equilibrium *via* a transient phosphinidene (Scheme 10). Interception of this phosphinidene was achieved by reaction of Cp*$_2$Zr(PH(C$_6$H$_2$Me$_3$))$_2$ with MeCN. The products included free phosphine and a six membered metallocycle Cp*$_2$Zr(NCMe)$_2$P(C$_6$H$_2$Me$_3$).

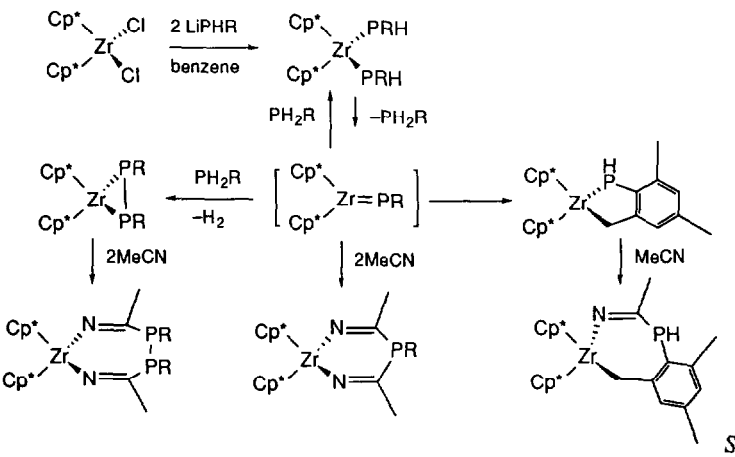

Scheme 10

The reaction of Cp$_2$ZrCl$_2$ with the corresponding lithium phosphinomethanides yields [Cp$_2$Zr(Cl)C-(PMe$_2$)(X)(Y)] (X = H, Y= PMe$_2$; X = H, Y = SiMe$_3$; X = Y = SiMe$_3$) which were obtained as crystalline solids and characterised by spectroscopy and X-ray structure determinations. All three complexes crystallise in a monoclinic space group and have in common a

metallaphosphacyclopropane ring with almost identical Zr-P, Zr-Cl and Zr-D (D = centroid of the Cp ring) distances. Due to the increasing steric congestion on going from $[Cp_2Zr(Cl)C\text{-}(PMe_2)(X)(Y)]$ (X = H, Y= PMe_2) to $[Cp_2Zr(Cl)C\text{-}(PMe_2)(X)(Y)]$ (X = Y = $SiMe_3$), the Zr-C(1) distances differ considerably $[Cp_2Zr(Cl)C\text{-}(PMe_2)(X)(Y)]$ (X = H, Y= PMe_2) 2.413(2)/2.408(2)Å; $[Cp_2Zr(Cl)C\text{-}(PMe_2)(X)(Y)]$ (X = H, Y = $SiMe_3$) 2.401(5)/2.423(5)Å; $[Cp_2Zr(Cl)C\text{-}(PMe_2)(X)(Y)]$ (X = Y = $SiMe_3$) 2.607(1)Å. $[Cp_2Zr(Cl)C\text{-}(PMe_2)(X)(Y)]$ (X = Y = $SiMe_3$) exists in solution as an η^1–(P)-coordinated 16 electron complex and decomposes above 0°C in solution (equ (7)). The complex $[Cp_2Zr(Cl)C\text{-}(PMe_2)(X)(Y)]$ (X = H, Y= PMe_2) exists in solution as a mixture of isomers, one of which exhibits a chelating P,P-coordination of the diphosphinomethanide ligand which forms a four-membered Zr-P-C-P heterocycle. The phosphorus nuclei of these two isomers equilibrate at elevated temperatures *via* a common intermediate (Figure 9) [36].

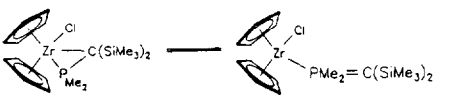

(7)

Reproduced with permission from ref. [36].

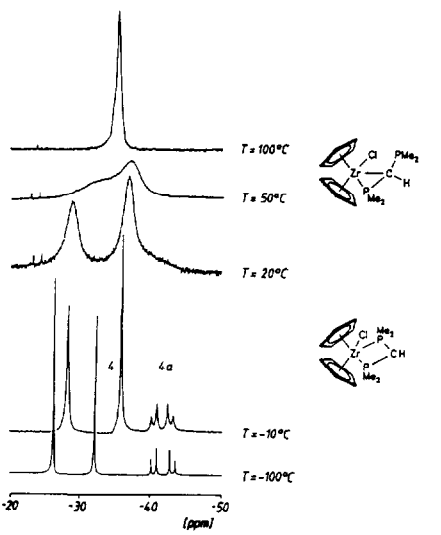

Figure 9. $^{31}P\{^1H\}$ NMR spectra of $Cp_2(Cl)Zr[(Me_2P)_2CH]$ at various temperatures. Reproduced with permission from ref. [36].

Several novel four-membered chelate complexes have been prepared from Cp_2ZrCl_2 and the appropriate lithium diphosphinomethanides in Et_2O (equ (8)). The solid state structures of $Cp_2(Cl)Zr[(Me_2P)_2C(SiMe_3)]$ and $Cp_2(Cl)Zr[(Ph_2P)_2C(SiMe_3)]$ show that the $Cp_2(Cl)Zr$ moiety in each case is coordinated by the $[(R_2P)_2C(SiMe_3)]^-$ ligands *via* both P atoms (η^2(P,P)). The weakness of the Zr-P bonds and their inequivalence is apparent from the ^{31}P NMR spectra and the solid-state structures (2.844(5)/2.721(5) and 2.823(4)/2.719(5)Å for the two independent molecules

of the former and 2.852(1)/2.817(1)Å in the latter). Notably $Cp_2(Cl)Zr[(Ph_2P)_2CH]$ is not in equilibrium with its η^2–(C,P) coordinated complex, unlike $Cp_2(Cl)Zr[(PMe_2)CH]$ [37].

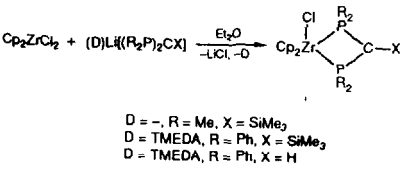

(8)

Reproduced with permission from ref. [37].

Addition of Cp_2ZrHCl to a thf solution of a phosphaimine at 0°C yields the three membered zirconaazaphosphiranes shown in Scheme 11. These probably result from the 1,2 addition of Cp_2ZrHCl to P=N followed by cyclization. Such cyclization is not observed for the equivalent reactions of Cp_2ZrH_2. The zirconaazaphosphiranes $\overline{RP(H)\text{-}NR'ZrCp_2(Cl)}$ (R = $(Me_3Si)_2N$, R' = $SiMe_3$; R = $(Me_3Si)(^tBu)N$, R' = ^tBu) undergo ring opening with $Fe_2(CO)_9$ or S_8 to give complexes of general formula R-P(H)XN(R')$ZrCp_2Cl$ (X = $Fe(CO)_4$, S). A similar reaction of $\overline{(Me_3Si)_2NP(H)N(SiMe_3)ZrCp_2(Cl)}$ with (trimethylsilyl)trifluoromethane sulfonate or methyltrifluoromethane sulfonate results in ring retention with the formation of a Zr-O covalent bond. Dissociation of this Zr-O bond occurs in polar solvents to give an ionic zirconium ring. Hydrozirconation of phosphaalkenes were also investigated. An easily accessible hydride-chloride exchange was observed for free or complexed halogenated phosphines and Cp_2ZrHCl (Scheme 12). The higher polarity of the P=N compared to the P=C bond led to unusual ligand exchanges and direct transformation of the zirconaphosphorane [38].

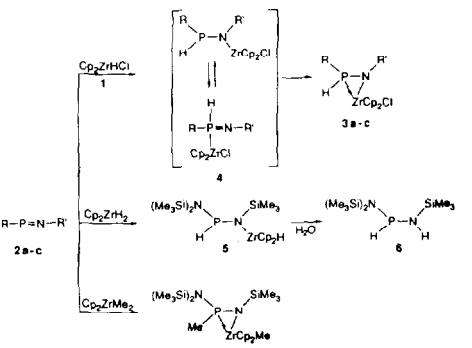

Scheme 11

Reproduced with permission from ref. [38].

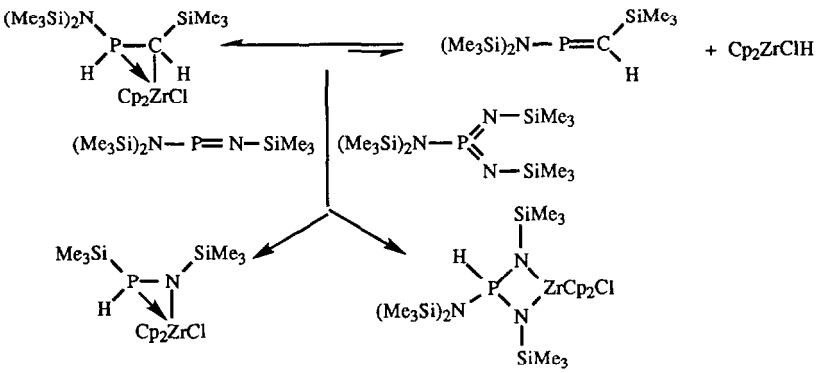

Scheme 12

The diene $[Zr(\eta^4\text{-}C_6H_8)(PMe_3)_2Cl_2]$ and the divalent compound $[Zr(\eta^6\text{-}C_6H_5Me)(PMe_3)_2Cl_2]$ have been synthesised from the reduction of $ZrCl_4$ using sodium amalgam in the presence of PMe_3 and cyclohexa-1,3-diene or toluene respectively. Variable temperature ^{31}P NMR spectra of the former imply that the phosphine ligands are *trans* to each other and that the diene is not bound symmetrically to the $Zr(PMe_3)_2Cl_2$ unit. The molecular structure of the toluene derivative has been confirmed by X-ray crystallography (Figure 10) [39].

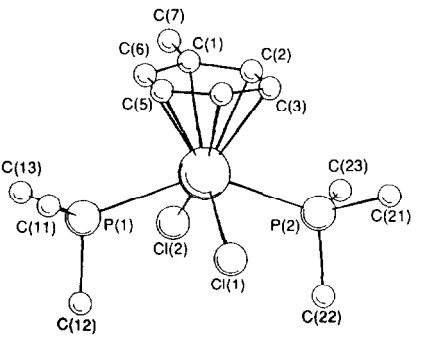

Figure 10. Molecular structure of $[Zr(\eta^6\text{-}C_6H_5Me)(PMe_3)_2Cl_2]$; only one molecule in the asymmetric unit is shown. The hydrogen atoms are omitted for clarity. Reproduced with permission from ref. [39].

The zirconium complexes $[Zr(\eta\text{-}C_7H_8)L_2Cl_2]$ (L = PMe_3, PMe_2Ph, $PMePh_2$) were also synthesised by the reduction of $ZrCl_4$ using Na/Hg in the presence of phosphine and cycloheptatriene. On reaction with lithium indenide these triene compounds give $[Zr(\eta\text{-}C_7H_7)(\eta^5\text{-}C_9H_7)]$ which subsequently react with PMe_3 to produce $[Zr(\eta\text{-}C_7H_7)(\eta^5\text{-}C_9H_7)(PMe_3)]$. Treatment of $[Zr(\eta\text{-}C_7H_8)(PMe_3)Cl_2]$ with sodium cyclopentadienide in thf at 60°C for 3 days gives $[\{Zr(\eta\text{-}C_5H_5)(\mu\text{-}\sigma\text{:}\eta^5\text{-}C_5H_4)(PMe_3)\}_2]$ but at room temperature gives $[Zr(\eta\text{-}C_5H_5)_2(\eta^2\text{-}C_7H_8)(PMe_3)]$ which exists in two isomeric forms. The major isomer was characterised by X-ray diffraction and found to have an η^2–3,4-C_7H_8 ligand. The minor isomer was tentatively assigned as having a η^2–1,2-C_7H_8 ligand from its ^{13}C NMR spectrum [40].

The compound (Z)-$Cp_2Zr\{C(Ph)=C(H)P(SiMe_3)_2\}Cl$ can be prepared from the regiospecific insertion of phenylacetylene into the Zr-P bond of $Cp_2Zr\{P(SiMe_3)_2\}Cl$. The compound was characterised by IR, ^1H NMR and ^{31}P NMR spectroscopy in solution and in the solid state by X-ray diffraction. On subsequent reaction of this species with MeLi or ^nBuLi the corresponding alkyl derivatives were prepared and in the methyl case an X-ray structure determination was carried out [41].

The dichloride Cp_2ZrCl_2 reacts with $Li(thf)_2PHCy$ to give $[Cp_2ZrP(Cy)P(Cy)P(Cy)]$. In solution this complex exists only in the *meso* forms. An X-ray structure determination revealed that the ZrP_3 ring is almost planar with near equivalent Zr-P bond lengths (2.618(4) and 2.628(4)Å) [42]. The reaction of $ZrCl_4(thf)_2$ with one equivalent of PR_3 (R = Cy, Ph, Me) results in the formation of $Cl_3Zr(\mu\text{-}Cl)_3ZrCl_2(PMe_3)_2$ and $[ZrCl_2(OCH_2CH_2CH_2CH_2PR_3)]_2$. These complexes were characterised spectroscopically (^1H, $^{13}C\{^1H\}$ and $^{31}P\{^1H\}$ NMR) and the molecular cores were confirmed by single crystal X-ray diffraction (Scheme 13). The mechanism for the formation of these complexes is thought to involve nucleophilic attack of the thf by the phosphines or substitution of the coordinated thf. It is interesting that neither the more sterically demanding phosphine PCy_3, nor the least basic, PPh_3, effect thf displacement [43].

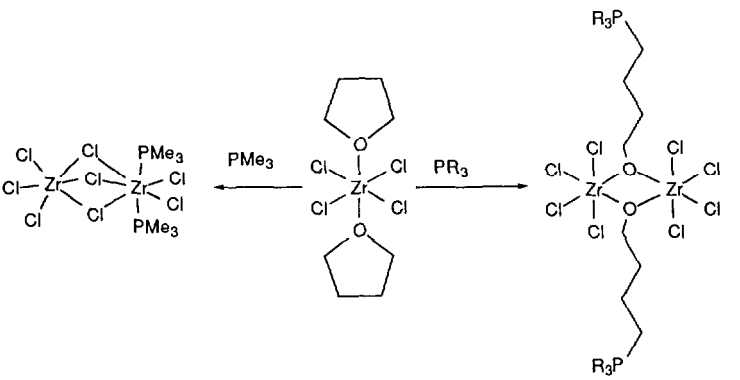

Scheme 13

Treatment of (η^2-ethene)(trimethylphosphane)zirconocene with 3,3-dimethylcyclopropene leads to the formation of a new type of bis(ethylzirconocene)complex with 3,3-dimethylallenediyl as a μ^1,μ^2-bridging ligand (equ (9)). It is proposed that the reaction occurs *via* an intermediate dizirconated cyclopropene. The single crystal X-ray structure of the product shows the allenediyl ligand to be asymmetrically coordinated but the 200MHz ^1H and 50.5MHz ^{13}C NMR spectra at 30°C show only one set of ethyl and one set of Cp signals possibly implying the rapid exchange of each Cp(Et)-Zr fragment [44].

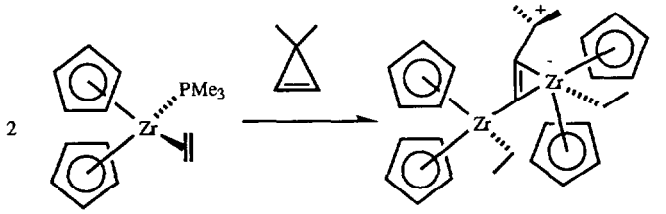

(9)

2.1.6 Complexes with oxygen donor ligands.

Oxozirconacyclohexadienes of general formula $Cp_2\overline{ZrOCH{=}CHCH{=}CR}$ were synthesised by the thermally induced σ,σ-exchange reactions of the furyl zirconocene complexes Cp_2ZrR(2-furyl) (R = Me, Ph, 2-furyl) (Scheme 14). When R = 2-furyl, this rearrangement follows first-order kinetics in the temperature range 140-180°C with $\Delta S^{\ddagger} = -9 \pm 5$ eu.

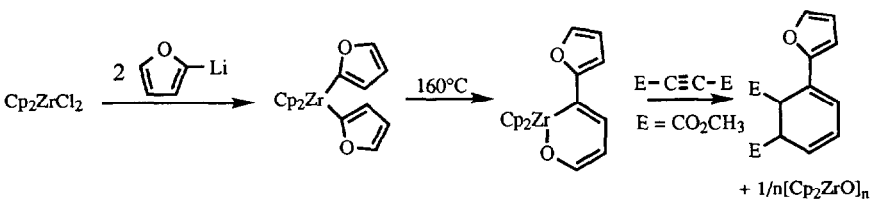

Scheme 14

The resulting 1,1-bis(η–cyclopentadienyl)-1-zircona-2-oxa-6-(2'-furyl)cyclohexa-3,5-diene was characterised by X-ray diffraction [45]. The $Cp_2Zr(SiMe_3)$(2-furyl) and $Cp_2Zr(SiMe_3)$(2-thienyl) complexes undergo the analogous dyotropic rearrangements far more quickly and for the latter $\Delta S^{\ddagger} = -12 \pm 5$ eu. The oxa and thiazirconacyclohexadienes $Cp_2\overline{Zr\text{-}X\text{-}CH{=}CHCH{=}C(SiMe_3)}$ (X = O, S) were characterised by X-ray diffraction and exhibit nonplanar metallacyclic conformations with the metal-chalcogen vectors significantly rotated relative to the planes of the indocyclic conjugated diene moieties (Figure 11) [46].

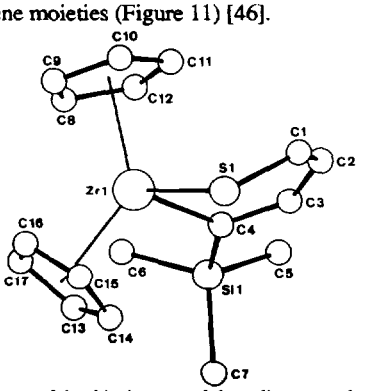

Figure 11. Molecular geometry of the thiazirconacyclohexadiene complex with (nonsystematic) atom numbering scheme. Reproduced from ref. [46] with permission.

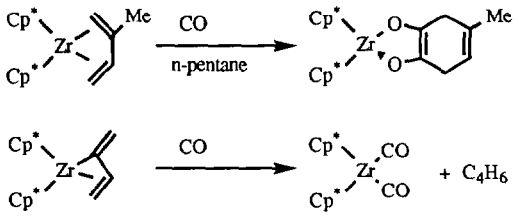

Scheme 15

Bis(pentamethylcyclopentadienyl)zirconium-(η^4–*S-cis*-diene) reacts with CO in pentane to give the mononuclear zirconium endiolates, whereas the *trans*-diene complexes react to give zirconocene-dicarbonyl complexes (Scheme 15). These compounds were characterised by IR, ^1H and ^{13}C NMR spectroscopy [47]. The ethylene complex $Cp_2Zr(C_2H_4)(PMe_3)$ reacts with tri- and tetra-functional H-acidic compounds under protonation of the ethylene ligand to form bridged trinuclear and tetranuclear ethyl complexes shown below (Scheme 16) [48].

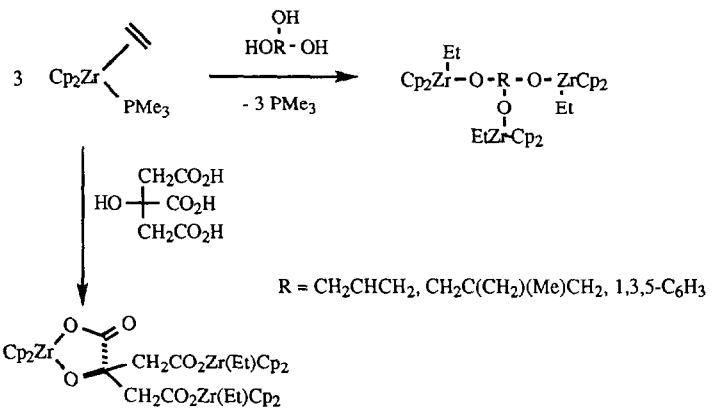

Scheme 16

Readily available zirconium intermediates i.e. $Cp_2Zr(H)Cl$ have been used to generate vinylic lithiocuprates. Introduction of an α,β-unsaturated ketone to these cuprates *in situ* generates the expected 1,4-adducts in good yields. This process can be applied to acetylenes which possess a nitrate, ester or chloride residue. The 5-hexynoic acid ethyl or methyl ester led only to olefinic products, possibly as a consequence of intra and or intermolecular chelation of the ester carbonyl with the Zr(IV) metal centre (Figure 12) [49].

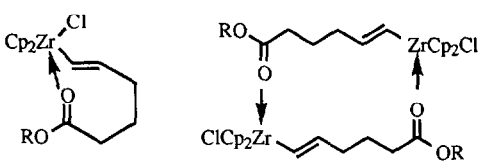

Figure 12

Ferrocenylmethanol ($FcCH_2OH$) is readily deprotonated using $NaN(SiMe_3)_2$ to give $Na[FcCH_2O]$. This ferrocenyl reagent reacts with Cp_2ZrCl_2 to give the alkoxide $Cp_2Zr(OCH_2Fc)_2$ which was characterised spectroscopically [50].

The dinuclear complex $Cp_2Zr(CH_2C_6H_5)[(\mu\text{-}OCH_2C_6H_5)Cr(CO)_3]$ was prepared from the stoichiometric reaction of $(HOCH_2C_6H_5)Cr(CO)_3$ and an alkylzirconocene compound (equ (10)). If a two molar equivalent of $(HOCH_2C_6H_5)Cr(CO)_3$ is used the resulting product is the trinuclear complex $Cp_2Zr[(\mu\text{-}OCH_2C_6H_5)Cr(CO)_3]_2$. These species have all been characterised by elemental analysis, IR, ^1H and ^{13}C NMR spectroscopy. The six $\nu(CO)$ stretches in the IR spectrum (nujol mull) of $Cp_2Zr[(\mu\text{-}OCH_2C_6H_5)Cr(CO)_3]_2$ indicated that the two $(\eta^6\text{–}C_6H_5)Cr(CO)_3$ moieties were different. This was confirmed by the single crystal X-ray structure (Figure 13) [51].

$$Cp_2Zr(CH_2C_6H_5)_2 + (HOCH_2C_6H_5)Cr(CO)_3 \longrightarrow Cp_2Zr(CH_2C_6H_5)[(\mu\text{-}OCH_2C_6H_5)Cr(CO)_3] + CH_3C_6H_5 \quad (10)$$

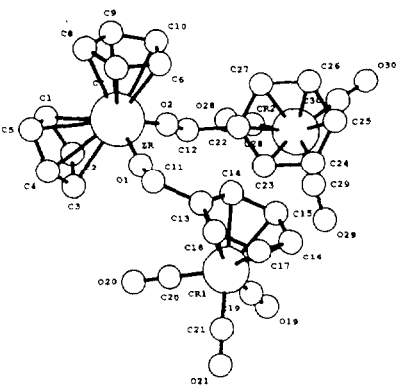

Figure 13. Molecular structure of $Cp_2Zr[(\mu\text{-}OCH_2C_6H_5)Cr(CO)_3]_2$. Reproduced with permission from ref. [51].

Benzoylacetone (bzacH) reacts with one equivalent of $Zr(OPr)_4$ to give the mono-substituted compound $(bzac)Zr(OPr)_3$, but with one equivalent of $Zr(O^tBu)_4$ to give $(bzac)_2Zr(O^tBu)_2$. Heating $(bzac)Zr(OPr)_3$ in the presence of $Cr(CO)_6$ led to the formation of a metal complex having a $Cr(CO)_3$ moiety π-bonded to the phenyl group of the benzoylacetonate ligand [52].

The reaction of dimethylzirconocene with 2*R*,3*R*-diethyl tartrate proceeds with the evolution of two equivalents of CH_4 to give a chiral diethyltartratozirconocene dimer. The enantiomer of this compound is produced in almost quantitive yield from the reaction of $Cp_2Zr(CH_3)_2$ and 2*S*,3*S*-diethyltartrate. The dimer contains a dimetallatricyclic framework tetraoxadizirconatricyclo-[5.3.0.0.2,6]decane in solution as well as in the solid-state. In solution the complex undergoes intramolecular automerisation to yield a ten-membered metallacyclic intermediate. The reaction of dimethylzirconocene with *meso*-dimethyltartrate gives the (meso-dimethyltartrato)zirconocene dimer, both isomers of which possess dynamic dimetallatricyclic structures in solution and which can be crystallised from CH_2Cl_2 [53].

The complex $[Cp^*_2Zr{=}O]$ has been synthesised at 160°C by α–elimination of benzene from $Cp^*_2Zr(Ph)(OH)$. The reaction of this species with a variety of unsaturated moieties was undertaken and the products characterised in the solid state by single crystal X-ray diffraction (Scheme 17). Kinetic, alkyne-exchange and isotope-labelling studies imply that the rearrangement of the oxametallacyclobutenes proceed *via* initial reversion of the metallacycle to an oxo-alkyne complex followed by attack of oxygen on the phenyl ring of the alkyne. $[Cp^*_2Zr{=}O]$ was also successfully synthesised at room temperature by deprotonation of $Cp^*_2Zr(OH)(OSO_2CF_3)$ with $KN(SiMe_3)_2$, and subsequently trapped by a variety of alkynes and nitriles. The isoelectronic $[Cp^*_2Zr{=}S]$ sulfido complex was also generated by the dehydrohalogenation of $Cp^*_2Zr(SH)(I)$ at room temperature. It can be isolated in pure form by its adducts $[Cp^*_2(L)Zr{=}S]$ (L = pyridine, 4-^{t}butylpyridine). The latter was crystallographically determined. This species undergoes similar reactions with unsaturated moieties (Scheme 18) [54].

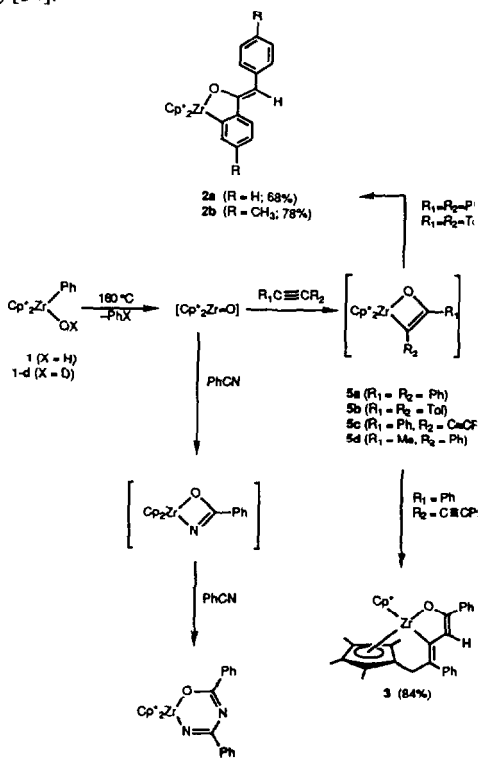

Scheme 17

Reproduced with permission from ref. [54].

The compound $(^tBuC_5H_4)_2Zr(C_5H_4)_2Fe$ is extremely resistant to chemical attack e.g. towards protic reagents. However it is possible to synthesise some zirconocenes of the general formula $(^tBuC_5H_4)_2Zr(X)(C_5H_4)Fe(C_5H_5)$ (X = OH, O-2,6-$Me_2C_6H_3$, O-3,5-$Me_2C_6H_3$, OCOPh) and subsequently $(^tBuC_5H_4)_2Zr(OR)_2$ (R = CH_3, CH_2Ph, *di*OMe-3,5-$PhCH_2$, COPh). UV Photolysis of $(^tBuC_5H_4)_2Zr(C_5H_4)_2Fe$ in the presence of PhS_2Ph or $PhSe_2Ph$ gave the

spectroscopically characterised systems, (^{t}BuC$_5$H$_4$)$_2$Zr(EPh)[(C$_5$H$_4$)Fe(C$_5$H$_4$)EPh] (E = S, Se) [55].

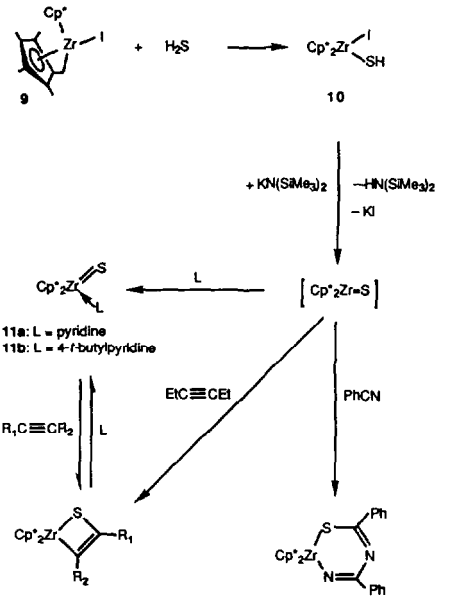

Scheme 18

Reproduced with permission from ref. [54].

A 2:1 mixture of (NaO$_2$CC$_5$H$_4$)Fe(CO)$_2$(CH$_2$C$_6$H$_5$) and Cp$_2$ZrCl$_2$ was stirred in dichloromethane at 0°C for 12 hours. The resulting complex [(η^5–C$_5$H$_5$)$_2$Zr(μ-O$_2$CC$_5$H$_4$)Fe(CO)$_2$(CH$_2$C$_6$H$_5$)]$_2$ was characterised by elemental analysis, IR, ^{1}H and ^{13}C NMR spectroscopy. The IR spectroscopic data (nujol mull) imply that one of the carboxylate groups is monodentate ($\nu(CO_2)_{asym}$ ~1643cm^{-1}, $\nu(CO_2)_{sym}$ ~1325cm^{-1}) and the other is didentate ($\nu(CO_2)_{asym}$ ~1529cm^{-1}, $\nu(CO_2)_{sym}$ ~1408cm^{-1}). Low temperature ^{13}C spectroscopic NMR (–90°C) spectra indicate fast interconversion between these monodentate and didentate carboxylate groups [56]. Some mixed metal-ligand peroxo complexes of general formula Zr(O$_2$)LL' were prepared (H$_2$L = diphenic acid, homophthalic acid, L' = 2,2'-bipyridine, 1,10-phenanthroline). The oxidation reactions of these systems with PPh$_3$ and AsPh$_3$ were examined [57].

The synthesis and characterisation of a d^0 Zr(IV) surface complex $\equiv Si\text{-}O\text{-}ZrNp_3$ has been achieved by the reaction of tetra*kis*(neopentyl)zirconium and a partially dehydroxylated (at 500°C) SiO$_2$ surface. Characterisation of the product was obtained by elemental analysis, IR spectroscopy and ^{13}C MAS NMR spectroscopy [58]. Tentative steps in the thermal decomposition of ZrF$_2$(F$_3$C$_2$F$_2$CF$_2$CO$_2$)$_2$ have been proposed from TG and macroscale pyrolysis studies [59].

2.1.7 *Complexes with sulfur donor ligands.*

The reaction of [SiMe$_2$(C$_5$H$_4$)$_2$][CpZrH(μ-H)]$_2$ with S$_8$ in toluene yields a novel disulfido-bridged Zr(IV) complex [SiMe$_2$(C$_5$H$_4$)$_2$][CpZr(μ-S)]$_2$ and Me$_2$S. A similar Zr(III) product

$[SiMe_2(C_5H_4)_2][CpZr(\mu\text{-}Cl)]_2$ is formed on photolysis of $[SiMe_2(C_5H_4)_2][CpZrCl(\mu\text{-}H)]_2$ by the reductive elimination of H_2. Both these diamagnetic zirconocenophane compounds have been characterised by ^1H and ^{13}C NMR spectroscopic measurements, electron spectroscopy, elemental analysis and X-ray diffraction methods. In each case the central $Zr_2(\mu\text{-}X)_2$ core is nearly planar with the Zr-Zr interatomic separation being 3.5210(6)Å (X = S) and 3.3853(4)Å (X = Cl). Cleavage of the Zr-(μ-X)-Zr bridges was not observed on addition of PMe_3, CNMe or pyridine at 20-130°C. However the addition of PMe_3 or thf to the chloro-bridged species gave paramagnetic dinuclear Zr(III) adducts, (according to solution EPR), that probably contain $[SiMe_2(C_5H_4)_2][CpZrCl(thf)]_2$. The μ-Cl complex reacts with $Ph_3P{=}O$ or CO_2 with O atom abstraction to give $[SiMe_2(C_5H_4)_2][CpZrCl]_2(\mu\text{-}O)$ [60].

Protonolysis of $[Cp_2ZrCH_3(thf)][BPh_4]$ with one equivalent of ^{t}BuSH gave a new (thiolato) zirconocene cation $[Cp_2Zr(S\text{-}^tC_4H_9)(thf)][BPh_4]$ in 79% yield. The structure of the CH_2Cl_2 analogue was confirmed by X-ray crystallography. The thf ligand can be displaced by other stronger donors such as *N,N*-dimethylaminopyridine. This synthetic procedure is not of general use as more acidic arenethiols e.g. Ar = 3,5-dimethylphenyl, react to give a mixture of $Cp_2Zr(SAr)_2$, $Cp_2Zr(SAr)(CH_3)$, BPh_3 and benzene. The (thiolato)zirconocene cation is not isostructural with the congeneric *tert*-butoxy cation; the Zr-E-C (E = O, S) angles differ according to the hybridisation at E, and the Zr-S distance (2.4618(13)Å) indicates little double-bond character. The compound is thermally sensitive in thf solution and decomposes *via* S-C bond cleavage to $[Cp_2ZrS]_2$ and $[(CH_3)_3C][BPh_4]$ [61].

The reaction of $(MeCp)_2ZrCl_2$ in a solution of distilled water and acetylacetone, with three molar equivalents of $NaS_2CN(CH_2Ph)_2$ yields a precipitate of $[(CH_3C_5H_4)Zr(S_2CN(CH_2Ph)_2)_3]$, whose molecular formula was determined spectroscopically. From the crystallographic data it is apparent that molecules of this complex have pentagonal bipyramidal geometry with the zirconium atom attached to a symmetrically bound $\eta\text{-}CH_3C_5H_4$ ligand and three didentate *N,N*-dibenzyldithiocarbamate ligands (Figure 14). The asymmetric unit comprises of two crystallographically independent molecules that differ from each other in that the $\eta\text{-}CH_3C_5H_4$ group and five equatorial S atoms of one molecule have an approximately staggered conformation and in the other have an eclipsed conformation [62].

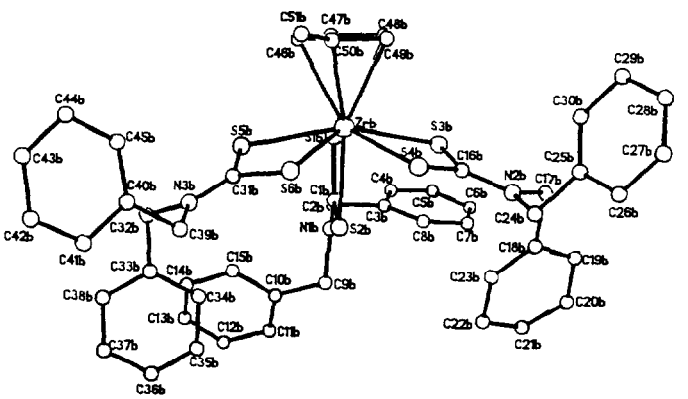

Figure 14. Molecular structure of $[(CH_3C_5H_4)Zr(S_2CN(CH_2Ph)_2)_3]$. Reproduced with permission from ref.[62].

The related complex $(RC_5H_4)_2Zr(S_2CN(CH_2Ph)_2)Cl$ (R = H, CH_3) were synthesised from the reaction of $(RC_5H_4)_2ZrCl_2$ with the anhydrous sodium salts of dibenzyldithiocarbamate. These compounds were characterised by elemental analysis, IR and ^1H NMR spectroscopy. The solid-state structure, determined using X-ray diffraction methods showed that $Cp_2Zr(S_2CN(CH_2Ph)_2)Cl$ has a five-coordinate bent metallocene geometry in which the zirconium atom is attached to two η^5–C_5H_5 groups, one didentate dibenzyldithiocarbamate ligand (Zr-S lengths 2.667(1)Å, 2.734(1)Å) and one chlorine atom (Zr-Cl length 2.549(1)Å) [63].

2.1.8 *Complexes with halide ligands.*

A systematic study of the third-order non-linear optical properties of some group 4 metallocene complexes Cp_2MX_2 has been undertaken (M = Ti, Zr, Hf; X = F, Cl, Br, CCC_6H_5). The third order nonlinear optical susceptibilities, γ, were derived from the third harmonic generation efficiencies determined for given solutions using a Raman shifted Nd:YAG laser with a fundamental of 1.9μm. In the metallocene-halide complexes the lowest lying absorptions in the UV-VIS spectra arise from Cp to metal charge-transfers. The third order susceptibilities however are too low to be measured accurately ($\gamma \sim 5 \times 10^{-36}$ esu). In the acetylide complexes γ ranged from 30×10^{-36} to 5×10^{-36} esu. The decreasing trend in γ values (Ti>Zr>Hf) is rationalised by assuming that the Ti *d* orbitals are closer in energy to the alkynyl π orbitals which leads to more significant mixing between them to form an extended π system [64].

Bis(pentamethylcyclopentadienyl)calcium reacts with $Cp^*_2ZrCl_2$ in toluene to yield 1:1 adducts in which the two bent metallocene units are bridged by a single μ-Cl, the remaining Cl remains terminal to the group 4 metal centre. The compound was characterised using standard spectroscopic techniques, and single crystal X-ray structural analysis. A similar reaction of Cp^*_2Ca and $Cp^*_2Zr(CO)_2$ resulted in a product whose spectroscopic data and elemental analysis indicated the formation of $Cp^*_2Ca(CO)_2ZrCp^*_2$. The ν(CO) stretches in the IR spectrum at 1939, 1844 and 1776 cm^{-1} indicate the presence of uncomplexed $Cp^*_2Zr(CO)_2$ and an isocarbonyl Ca···OC-Zr linkage [65].

The decomposition of a series of compounds $(C_5H_4R)_2ZrCl_2$ (R = H, Me, ^{n}Pr, ^{i}Pr, ^{n}Bu, ^{t}Bu) under electron impact has been studied. Direct evidence for the participation of hydrogen atoms at the substituemt α–carbon atom was obtained on the decomposition of $[C_5H_4C(D)Me_2]_2ZrCl_2$ which initially eliminates a DCl molecule. Subsequent abstraction of an HCl molecule is thought to result from deutero-hydrogen exchange or the participation of methyl groups in the substituent [66].

2.1.9 *Heterometallic complexes.*

(Butadiene)zirconocene reacts with 1 molar equivalent of $AlCl_3$ to give $Cp_2Zr(\mu\text{-}C_4H_6)(\mu\text{-}Cl)AlCl_2$, a chiral heterodimetallic complex containing a butadiene ligand in a novel coordination mode. The conjugated diene bridges the two metal atoms in an unsymmetrical fashion such that carbon atoms C(1) and C(2) are bound to the zirconium centre (Zr-C(1) = 2.348(2)Å, Zr-C(2) = 2.525(3)Å) and C(4) is bound to the aluminium atom (Al-C(4) = 1.966(2)Å). The remaining sp^2

C(3) of the butadiene ligand is not used in bonding (Zr-C(3) = 3.04Å). The C(2) to metal bonding coordination may be described as a π-agostic interaction. The compound was characterised in solution by ^{1}H and ^{13}C NMR spectroscopy, and in the solid state by X-ray diffraction (Figure 15). The structure shows a C(2), C(3) disorder, corresponding to the two enantiomers [67].

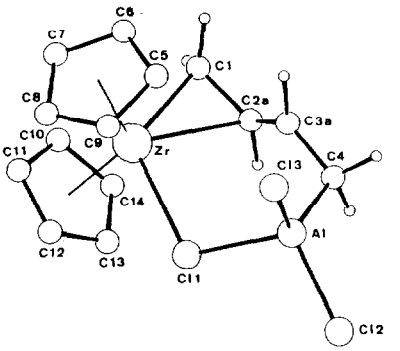

Figure 15. The molecular geometry of the major molecular isomer of $Cp_2Zr(\mu\text{-}CH_2CHCHCH_2)(\mu\text{-}Al)AlCl_2$. Reproduced with permission from ref. [67].

The Lewis acid diisobutylaluminium hydride reacts with reactive alkyne-zirconium complexes e.g. (η^2-aryne)$(PMe_3)ZrCp_2$ to give an $Me_3PHAl(^iBu)_2$ adduct which subsequently generates a (η^2–aryne)$ZrCp_2$ intermediate that is trapped by additional hydridoaluminium reagent to yield $Cp_2Zr(\mu\text{-}\eta^1\text{:}\eta^2\text{–}C_6H_4)(\mu\text{-}H)Al(^iBu)_2$. The latter has been structurally characterised using X-ray diffraction methods and has a planar -tetracoordinate carbon centre at the bridgehead position of the dimetallabicyclic framework. Using $AlMe_3$ or $AlEt_3$ structurally analogous complexes can be formed e.g. $Cp_2Zr(\mu\text{-}\eta^1\text{:}\eta^2\text{–}C_6H_4)(\mu\text{-}CH_3)AlMe_3$ or $Cp_2Zr(\mu\text{-}\eta^1\text{:}\eta^2\text{–}C_6H_4)(\mu\text{-}CH_2CH_3)AlEt_2$. A similar synthetic route from the stable (η^2–alkyne)metallocene complexes, (η^2–cyclohexyne)$(PMe_3)ZrCp_2$, or (η^2–diphenylacetylene)$(PMe_3)ZrCp_2$ gives the respective $Cp_2Zr(\mu\text{-}\eta^1\text{:}\eta^2\text{–}RCCR)(\mu\text{-}CH_3)AlMe_2$ products. The reaction between (η^2–tolane)$(PMe_3)ZrCp_2$ with a mixture of 9-BBN and BEt_3 produced $Cp_2Zr(\mu\text{-}\eta^1\text{:}\eta^2\text{–}PhC_2Ph)(\mu\text{-}H)BEt_2$ in low yield [68]. The structure of the related $Cp_2Zr(\mu\text{-}\eta^1\text{:}\eta^2\text{–}PhC_2Ph)(\mu\text{-}H)Al(^iBu)_2$ species has been determined using X-ray diffraction methods (Scheme 19) [69].

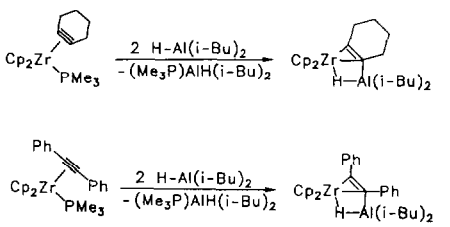

Scheme 19

Reproduced with permission from ref. [69].

Several examples of σ-hydrocarbyl-bridged dimetallabicyclic complexes of gallium and zirconium have been generated from the reaction of (η^2-alkyne)(PMe_3)$ZrCp_2$ with excess $GaMe_3$. The resulting products $Cp_2Zr(\mu\text{-}\eta^1{:}\eta^2\text{-}C_6H_8)(\mu\text{-}CH_3)GaMe_2$ and $Cp_2Zr(\mu\text{-}\eta^1{:}\eta^2\text{-}C_6H_4)(\mu\text{-}CH_3)GaMe_2$ contain a planar tetracoordinate carbon centre in the $\mu\text{-}\eta^1{:}\eta^2$-hydrocarbyl bridge, which forms a three centre-two electron bond with the attached metal centres. These compounds have been characterised from ^1H, ^{13}C NMR spectroscopy and X-ray crystallography. The ^{13}C NMR resonance of the planar tetracoordinate carbon (~δ117.3) compares well with that of the analogous zirconium/aluminum "anti-van't Hoff/Le Bel" complexes. Removal of the Me_3Ga unit can be achieved by reacting these compounds with norbornene or ethylene as in Scheme 20 to give five-membered metallacyclic products which have been spectroscopically characterised. A third product also postulated to contain a planar tetracoordinate C atom $Cp_2Zr(\mu\text{-}PhCCH)(\mu\text{-}Cl)GaMe_2$ is the result of the reaction of $Cp_2Zr(H)Cl$ with $PhCCGaMe_2$ and is thought to be produced in a similar manner *via* an (η^2-alkyne)zirconocene intermediate [70].

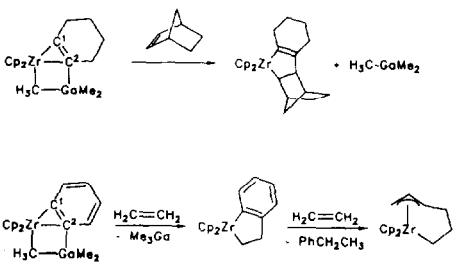

Scheme 20

Reproduced with permission from ref. [70].

The reaction of Zr(neopentyl)$_4$ with RfOH (Rf = $CH(CF_3)_2$) in a 1:4 molar ratio gives $Zr(ORf)_4$ which reacts with TlORf in a 1:2 molar ratio to give $Tl_2Zr(ORf)_6$ (Figure 16). The X-ray diffraction determination of the structure of this compound reveals a $Tl(\mu\text{-}ORf)_3Zr(\mu\text{-}ORf)_3Tl$ connectivity based on a distorted octahedral $Zr(ORf)_6^{2-}$ substructure. The molecule is rigorously centrosymmetric, so that the Tl/Zr/Tl unit is linear. The ^{19}F NMR and ^{205}Tl NMR spectra show Tl/F nuclear spin coupling and imply that there is direct bonding involved between the fluorine and thallium atoms. Variable temperature NMR spectroscopic studies have revealed that there is a fluxional process occurring in solution which corresponds to an intramolecular migration of the Tl centres over all the ZrO_3 triangular faces within the molecule [71].

To a solution of $Cp''_2Zr(^nBu)_2$ prepared *in situ* from ^{n}BuLi and Cp''_2ZrCl_2 (Cp'' = Cp, Cp^*) was added two equivalents of $Sn(CH(SiMe_3)_2)_2$. The product $Cp^*_2Zr\{Sn(CH(SiMe_3)_2)_2\}_2$ was characterised by ^{119}Sn NMR spectroscopy, which gives an upfield resonance at δ 1678 relative to Me_4Sn with ^{117}Sn satellites arising from an adjacent ^{117}Sn nucleus ($^2J^{117}Sn^{119}Sn$ = 630Hz). An X-ray crystal structure of $Cp^*_2Zr\{Sn(CH(SiMe_3)_2)_2\}_2$ reveals that the molecule has pseudo-tetrahedral geometry about the zirconium atom (Figure 17). The Zr-Sn bonds are equivalent (2.8715(11)Å), which compared to a related Zr(II) complex $[(Ph_3Sn)_4Zr(CO)_4]^{2-}$ (Zr-Sn 3.086Å)

appears short. This and extended Hückel MO calculations imply considerable π-bonding between the zirconium and the tin. The "Cp_2Zr" carbene-like fragment contains an extra low-energy orbital which allows it to couple with a second stannylene donor despite the steric bulk of the stabilising alkyl groups on the tin atoms. There is no tin-tin bonding interaction (4.236Å) [72].

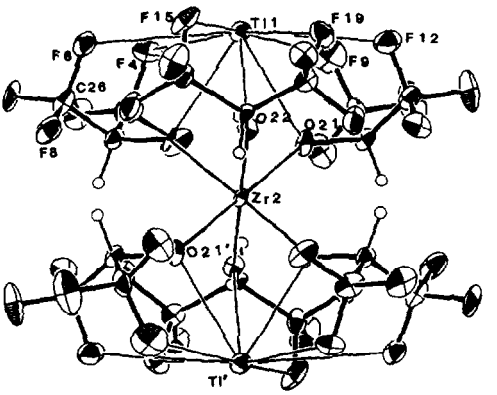

Figure 16. ORTEP drawing of $Tl_2Zr(OCH(CF_3)_2)_6$. Thermal ellipsoids are drawn at the 50% probability level. Reproduced with permission from ref. [71].

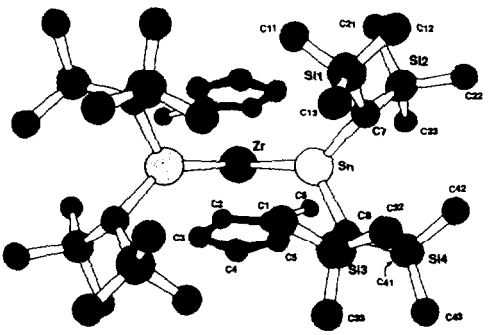

Figure 17. Chem 3D diagram and atom-numbering scheme for $Cp_2Zr\{Sn[CH(SiMe_3)_2]_2\}_2$. Reproduced with permission from ref. [72].

A series of triphenylsilyl, triphenylgermyl and triphenylstannyl derivatives of zirconocene and hafnocene were synthesised, using the novel reaction of $LiEPh_3(thf)_3$ (Scheme 21). The methyl derivatives of $Cp^*_2Zr(SiPh_3)Cl$ and $Cp^*_2Hf(SiPh_3)Cl$ were prepared by reaction with MeMgBr and hydrogenation of the same species gave the metal hydrides. The stannyl and germyl complexes were found to be less reactive towards hydrogen. σ-bond metathesis reactions with hydrogen and phenylsilane and insertion reactions with carbon-monoxide and 2,6-$Me_2C_6H_3NC$ established the reactivity trends M-$SiPh_3$>M-$GePh_3$>M-$SnPh_3$ [73].

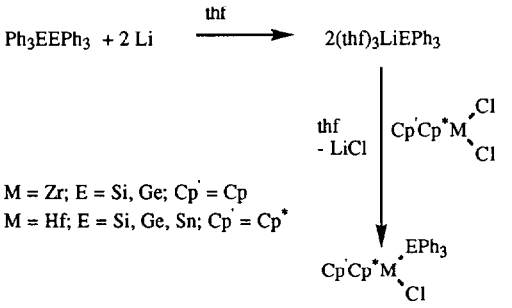

Scheme 21

The compound $[Me_2GeS]_3$ reacts with $(^tBuCp)_2ZrPh_2$ *via* a mechanism that is thought to involve insertion of [Me2Ge=S] into the Zr-C bond of a transient benzynezirconocene, $(^tBuCp)_2Zr(\eta^2\text{-}C_6H_4)$. The resulting dimetallacycle $[(^tBuCp)_2\overline{Zr\text{-}S\text{-}Ge(Me)_2(o\text{-}C_6H_4)}]$ is very similar to the crystallographically characterised product $[Cp_2\overline{Zr\text{-}S\text{-}Ge(Me)_2(o\text{-}C_6H_4)}]$ from the reaction of $[Me_2GeS]_3$ with $Cp_2Zr(CH_3)C_6H_5$ [74].

$$[M(ER)_2]_n \longrightarrow [ME]_n + nER_2 \quad (11)$$

M = Zn, Cd, Hg
E = S, Se, Te
R = aryl, alkyl

Metal chalcogenolates are known to decompose to chalcogenides (equ (11)). Analogous reactivity is observed in homogeneous solutions. Homoleptic tellurolates of Zr and Hf were prepared as shown in Scheme 22. The complexes $(TeSi(SiMe_3)_3)_4M$ were characterised by single crystal X-ray crystallography and ^1H, $^{13}C\{^1H\}$ and $^{125}Te\{^1H\}$ NMR spectroscopy. These compounds are *pseudo*tetrahedral e.g. Te-Zr-Te angles vary from 101.63(2)° to 115.89(2)°. They readily react with Lewis bases, but the product from the reaction with two equivalents of dmpe results in a clean transformation to a seven coordinate metal telluride (Figure 18). The X-ray data on these telluride complexes show the phosphorus atoms to be transoid and the NMR spectroscopic data show that the molecule is undergoing a fluxional process in solution. The tellurolate ligands have Zr-$TeSi(SiMe_3)_3$ bond distances of 2.939(1)Å and 3.028(1)Å for axial and equatorial sites and the Zr-Te interaction is short at 2.650(1)Å [75].

The hydride elimination reaction between R_4Zr (R = $PhCH_2$, Me_2N, Et_2N) and $HCo(CO)_3(L)$ (L = CO, PPh_3) and the salt elimination reaction between R'_3ZrX (R' = $PhCH_2$, Me_2N, Et_2N, ^iPrO, ^nBuO; X = Br, Cl) and $Na[Co(CO)_4]$ produced a series of dimetallic and trimetallic compounds, for example $(PhCH_2)_3ZrCo(CO)_3(L)$ and $(PhCH_2)_2Zr[Co(CO)_3(L)]_2$. The products were characterised by elemental analysis, IR and ^1H NMR spectroscopy [76].

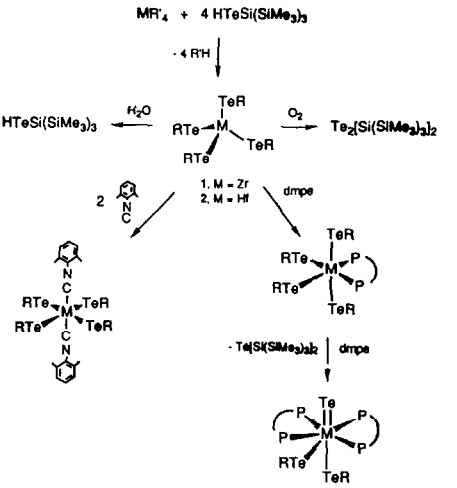

Reproduced with permission from ref. [75].

Scheme 22

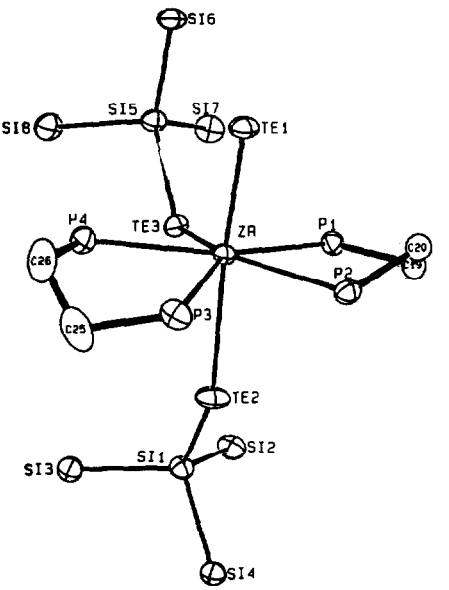

Figure 18. ORTEP view of ZrTe[TeSi(SiMe3)3]2(dmpe)2 with thermal ellipsoids at 50% probability. Methyl groups are omitted for clarity. Reproduced with permission from ref. [75].

Two predominant competing reactions are observed for $Cp(PMe_3)_2RuCH_2CH_2ZrClCp_2$ and $Cp(PMe_3)_2RuCH{=}CHZrClCp_2$. These are the insertions reactions of unsaturated organic molecules e.g. CO_2, ^tBuCN, into the Zr-C bond, (equ (12)) and β-hydride elimination (Scheme 23). Complexes $Cp(PMe_3)_2RuCCZrClCp_2$ and $Cp(PMe_3)_2RuCH_2CH_2ZrClCp_2$ react with ^tBuCN and benzophenone to give the following insertion products, an η^2-iminoacyl

$Cp(PMe_3)_2RuCCC(N^tBu)ZrClCp_2$ and $Cp(PMe_3)_2RuCH_2CH_2CPh_2OZrClCp_2$ respectively. In an excess of ^nBuCCH, β-elimination is observed from $Cp(PMe_3)_2RuCH{=}CHZrClCp_2$ to give $Cp(PMe_3)_2RuCCH$ and $Cp_2Zr(Cl)CH{=}CH^nBu$ [77].

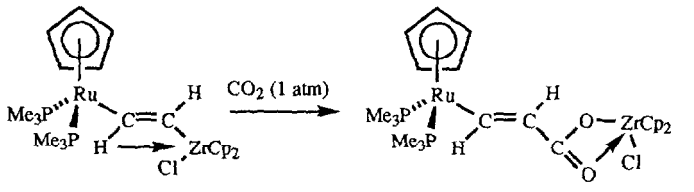

(12)

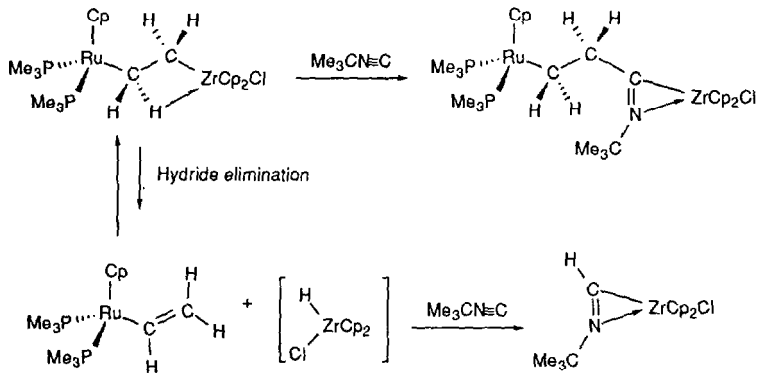

Scheme 23

2.2 ZIRCONIUM(III)

2.2.1 Complexes with hydride ligands

The reaction of $Cp_2ZrCl(CH_2PPh_2)$ with $LiAlH(O^tBu)_3$ or $NaAlH_2(OCH_2CH_2OMe)_2$ gives the hydride $[Cp_2ZrH(CH_2PPh_2)]_n$. The latter undergoes reduction with sodium naphthalenide to give a Zr(III) complex which was characterised by its ESR spectra to be $CpZr(\eta^2{-}CH_2PPh_2)_2$. This reaction is thought to involve redistribution of $[Cp_2ZrH(CH_2PPh_2)]^-$ (Scheme 24). Thermolysis of $[Cp_2ZrH(CH_2PPh_2)]_n$ at 60°C and subsequent ^1H and $^1H\{^{31}P\}$ spectra indicated that different Zr(III) complexes, "Cp_2ZrH" and $[Cp_2Zr(\eta^2{-}CH_2PPh_2)]$ were produced supposedly *via* reductive elimination of CH_3PPh_2 and the decomposition of a transition homodimetallic complex $[Cp_2Zr(\mu\text{-}H)(\mu\text{-}CH_2PPh_2)ZrCp_2]$. Evidence for this mechanism comes from the reaction of $[Cp_2ZrH(CH_2PPh_2)]_n$ with butadiene which gives $Cp_2Zr(\eta^4{-}$butadiene) *via* a $[Cp_2Zr(\mu\text{-}CH_2PPh_2)(\mu\text{-}CH{=}CHCH_2CH_3)ZrCp_2]$ intermediate [78].

$$(1/n)[Cp_2ZrH(CH_2PPh_2)]_n \xrightarrow{Na(np)} [Cp_2ZrH(CH_2PPh_2)]^- + Na^+ + Np$$

$$[Cp_2ZrH(CH_2PPh_2)]^- \longrightarrow {}^1/_2[Cp_2ZrH_2]^- + {}^1/_2[Cp_2Zr(CH_2PPh_2)_2]^-$$

$${}^1/_2[Cp_2Zr(CH_2PPh_2)_2]^- \longrightarrow {}^1/_2[Cp_2Zr(\eta^2\text{-}CH_2PPh_2)_2]^- \; (+{}^1/_2Cp^-)$$

Reproduced with permission from ref. [78].

Scheme 24

$$[Cp'_2ZrCH_3]^+[CH_3B(C_6F_5)_3]^- \xrightarrow[-\,CH_4]{H_2/pentane} [Cp'_2ZrH]^+[CH_3B(C_6F_5)_3]^-$$

$$[Cp'_2ZrH]^+[CH_3B(C_6F_5)_3]^- \xrightarrow{H_2/C_6H_6,\; -\,CH_4} [Cp'_2ZrH]^+[HB(C_6F_5)_3]^-$$

$$[Cp'_2ZrH_2] + B(C_6F_5)_3 \xrightarrow[benzene]{pentane\ or} [Cp'_2ZrH]^+[HB(C_6F_5)_3]^-$$

Scheme 25

The first base-free cationic zirconocene hydrides have been prepared by two routes; hydrogenolysis and hydride abstraction (Scheme 25). These two cationic hydrides have been spectroscopically characterised and a X-ray crystal structure determination of $[Cp'_2ZrH]^+[CH_3B(C_6F_5)_3]^-$ confirms that this system has a bent-sandwich structure with a weakly coordinating $[HB(C_6F_5)_3]^-$ ion, with no involvement of a B-H functionality coordinating to the metal (Figure 19). There are weak but significant Zr...F-C interactions (Zr-F(1) = 2.416(3)Å, Zr-F(2) = 2.534(3)Å). Both hydrides have been shown to be active homogeneous catalysts for the polymerisation of ethene and propene [79].

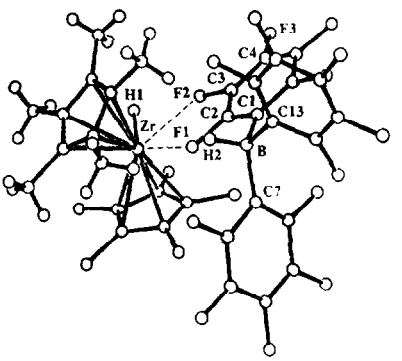

Figure 19. Molecular structure of $[Cp'_2ZrH]^+[CH_3B(C_6F_5)_3]^-$. Only one of the two possible orientations of the disordered Cp' ring is shown. Reproduced with permission from ref. [79].

2.2.2 Complexes with coordinating carbon ligands

The reaction of the Zr(III) complex $[\{(\eta^5\text{-}C_5H_5)Zr(\mu\text{-}Cl)\}_2(\mu\text{-}\eta^5\text{:}\eta^5\text{-}C_{10}H_8)]$ with LiCCPh gives a compound with each CCPh unit σ coordinated to one Zr atom and π coordinated to another (equ (13)). The evidence for this type of interaction was obtained from the ^{13}C NMR spectroscopic resonances of the acetylene C_α and C_β carbon nuclei (δ 211.2(s) C_α, δ 144.0(t) J_{CH} = 4.57Hz, C_β) which are similar to those observed for dinuclear complexes of the type $(Cp_2Zr)_2(CCR)_2$. The same Zr(III) starting material reacts with 2,6-dimethylphenyl isocyanide to give a dimeric imine complex which can be alkylated with MeLi. The subsequent dimethyl derivative was studied by X-ray diffraction (Scheme 26) [80].

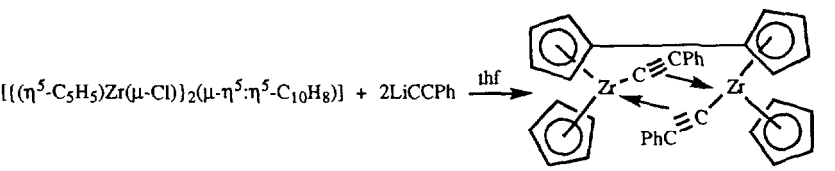

(13)

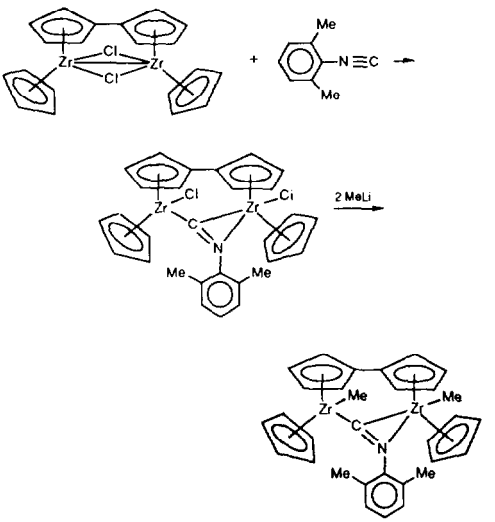

Reproduced with permission from ref. [80].

Scheme 26

2.2.3 Complexes with nitrogen donor ligands

The reaction of four equivalents of LiNHAr (Ar = 2,6-$C_6H_3{}^iPr$) with a solution of $ZrCl_4(thf)_2$ in thf/pyridine yields $Zr(=NAr)(NHAr)_2(py)_2$ in high yield. This complex reacts with one and two equivalents of Me_3SiCl to give $Zr(=NAr)(NHAr)Cl(py)_2$ and $Zr(=NAr)Cl_2(py)_3$ respectively. The former reacts with one equivalent of $K[N(SiMe_3)_2]$ to produce $Zr(=NAr)(NHAr)[N(SiMe_3)_2](py)_2$ which could not be converted to the bis(imido) species.

Investigations into the reactivity of the complex $Zr(=NAr)Cl_2(thf)_2$ led to the formation of $[(\eta^5\text{-}C_5H_4Me)Zr(=NAr)Cl]_2$ which has been structurally determined by X-ray crystallography. The compound has a dimeric structure with bridging imido ligands one of which adopts an unusual μ-$[\eta^1(N):\eta^2(N,C)]$ imido binding mode (Scheme 27) [81].

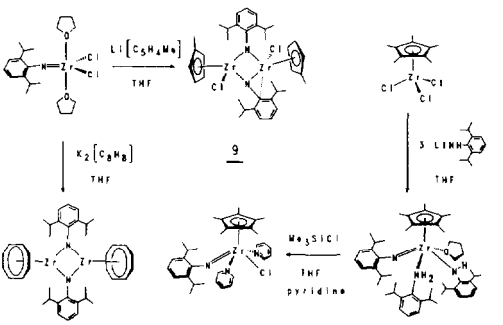

Reproduced with permission from ref. [81].

Scheme 27

The reaction of four equivalents of 4-tert-butylpyridine or 4-(1-butylpentyl)pyridine to a slurry of $[ZrCl_3(P\text{-}^nBu_3)_2]_2$ in hexanes gives $ZrCl_3(py\text{-}R)_2$ according to equation (14). The ^1H NMR spectroscopic data are consistent with a diamagnetic Zr-Zr bonded compound and reveal only one type of pyridine. An X-ray structure determination of the 4-(1-butylpentyl)pyridine derivative confirms this formulation (Figure 20). The reaction of one equivalent of trimethylacetonitrile with $[ZrCl_3(py)_2]_2$ in benzene gives 92% $Zr_2Cl_6(py)_3(^tBuCN)$ after work-up. An X-ray crystal structure determination of this compound shows the nitrile ligand to be σ,π-coordinated. At 1.255(9)Å the C-N bond distance of the coordinated nitrile is longer than that of free nitrile, and the Me-C-C-N angle (127.4(7)Å) is close to the value expected for sp^2 hybridisation. This and the Raman spectroscopic data imply that there is significant population of the π^* orbitals of the nitrile [82].

$$[ZrCl_3(P^nBu_3)_2]_2 + 4\ pyR \xrightarrow[1\ h]{\text{hexanes}} [ZrCl_3(pyR)]_2 + 4\ P^nBu_3$$

$$R = H, 4\text{-}^tBu, 4\text{-}(1\text{-butylpentyl}) \qquad (14)$$

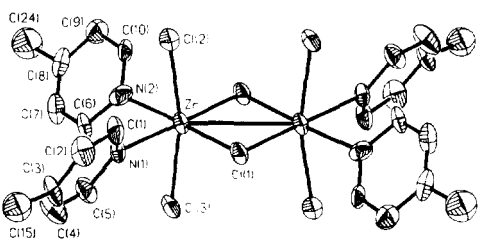

Figure 20. Plot of $[ZrCl_3(4\text{-}(1\text{-butylpentyl})pyridine)_2]_2$, showing the atom-numbering scheme (30% probability ellipsoids). The heavily disordered aliphatic chains on the pyridines have been omitted.
Reproduced with permission from ref. [82].

2.2.4 *Complexes with phosphorus donor ligands*

The reaction of Cp_2ZrCl_2 with two equivalents of ^nBuLi yields *in situ* "Cp_2Zr". The addition of $PhPH_2$ results in P-H activation and the formation of an intermediate, $Cp_2Zr(PPhH)H$. The Lewis acidity of this intermediate invokes C-H activation in the ancillary cyclopentadienyl ligands and subsequent C-C bond formation to give $[(\eta^5\text{-}Cp)Zr(\mu^2\text{-}PPhH)(\mu\text{-}\eta^5\text{:}\eta^5\text{-}C_5H_4C_5H_4)]_2$ which has been spectroscopically and crystallographically characterised. This dimeric Zr(III) species contains CpZr moieties which are bridged by two phenylphosphido groups and a slightly bent (7.9° between the planes of the rings) fulvalenide moiety. The observed diamagnetism of this complex is consistent with anti-ferromagnetic coupling of the Zr(III) centres which are 3.549(2) Å apart. If a similar reaction using $(2,4,6\text{-}^tBu_3C_6H_2)PH_2$ is employed, the isolated product is a trimeric, phosphide-capped Zr(IV) species, $[(\eta^5\text{-}Cp)(\mu\text{-}\eta^1\text{:}\eta^5\text{-}Cp)Zr_3(\mu^3\text{-}P)]$. The crystal structure of this species provides the first structural precedent for $\eta^1\text{:}\eta^5$-cyclopentadienyl groups between Zr centres, a feature of the proposed intermediate in the formation of $[(\eta^5\text{-}Cp)Zr(\mu^2\text{-}PPhH)(\mu\text{-}\eta^5\text{:}\eta^5\text{-}C_5H_4C_5H_4)]_2$ (Scheme 28) [83].

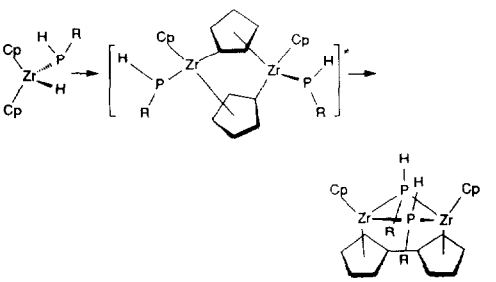

Reproduced with permission from ref. [83]. *Scheme 28*

2.2.5 *Complexes with halide ligands*

Crystalline paramagnetic dinuclear zirconocene(III) complexes have been synthesised (Scheme 29). Single crystal X-ray analysis of the chlorine derivatives show that in each case the two $[\eta\text{-}C_5H_3(SiMe_3)_2\text{-}1,3]$ rings are staggered. $[\{Zr(\eta\text{-}C_5H_3(SiMe_3)_2\text{-}1,3\}_2(\mu\text{-}X)\}_2]$ (X = Cl, Br) have characteristic Zr(III) ESR spectra (PhMe, 300K) and exceptionally long Zr...Zr contacts (3.86 - 4.14Å). The Cl dimer undergoes nucleophilic bridge-cleavage addition reactions with Cl^- ions and forms weak adducts with PMe_3 or thf according to the equilibrium (equ (15)) [84].

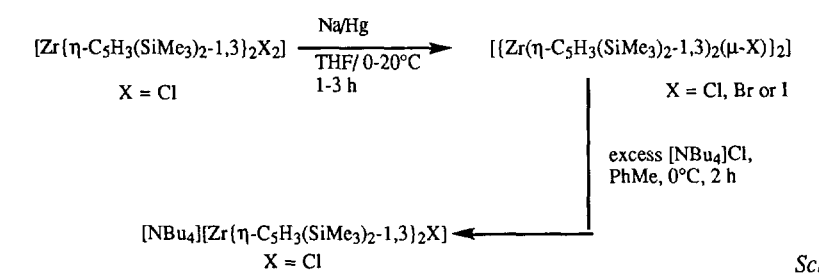

Scheme 29

$$[\{Zr(\eta\text{-}C_5H_3(SiMe_3)_2\text{-}1,3)_2(\mu\text{-}Cl)\}_2] + 2\,L \underset{L = PMe_3,\ thf}{\rightleftharpoons} 2\,[Zr\{\eta\text{-}C_5H_3(SiMe_3)_2\text{-}1,3\}_2(Cl)(L)] \quad (15)$$

2.3 ZIRCONIUM(II)

2.3.1 Complexes with nitrogen donor ligands

The reaction of (5,10,15,20-tetraphenylporphinato)zirconium diacetate (TPP)Zr(OAc)$_2$ with organolithium or Grignard reagents gives the corresponding σ-bonded organozirconium(IV) porphyrins (TPP)ZrR$_2$ (R = Me, Et, ^{n}Bu, Ph). Even those species with β–hydrogen atoms present on the substituents are stable at room temperature. Irradiation (>420nm) of a C_6D_6/Et_2O solution of (TPP)ZrMe$_2$ for 3 hours produced a new Zr(II) porphyrin complex which is stabilised by ether coordination. Evidence for this species is obtained from the ^{1}H NMR spectra which shows the disappearance of the Zr-Me groups (δ −2.98) and a single resonance for the *ortho* protons of the peripheral phenyl rings (δ 8.64). The coordinated ether molecules were displaced by 1-methylimidazole and the complex was readily demetallated by H_2O to give $TPPH_2$ [85].

The di(π-radical cation) complex $[Zr(TPP)_2][SbCl_6]_2$ was synthesised from the reaction of $Zr(TPP)_2$ and phenoxathiinylium hexachloroantimonate in CH_2Cl_2 at room temperature. Spectroscopic and magnetic susceptibility data on the dication complex indicate strong antiferromagnetic coupling between the unpaired electrons on the two porphyrin rings. The solid-state structures of the series $[Zr(TPP)_2]$, $[Zr(TPP)_2][SbCl_6]$ and $[Zr(TPP)_2][SbCl_6]_2$ is now complete and confirms that the π-π interaction between the two porphyrin rings is enhanced by oxidation. The near IR band (780nm, fwhm = 130nm) for $[Zr(TPP)_2]^{2+}$ is blue-shifted compared to the monocation $[Zr(TPP)_2]^+$, (1 10nm). Similar blue-shifts have been observed for actinide and lanthanide, two-hole and single-hole complexes [86].

The molecular structure of Zr(OEP)$_2$ has been elucidated by an X-ray structural analysis. Single crystals were obtained by slow diffusion of DMSO into a toluene solution of Zr(OEP)$_2$. The two OEP rings are parallel and rotated by an angle of ~45° with respect to their eclipsed position. The zirconium atom is located 127.1 and 126.0 pm above the mean planes of the nitrogen atoms of the two OEP rings, and 162.7 and 157.8 pm above their 24-atom-core mean planes respectively. These values are 1.3 to 6.6 pm shorter than the corresponding values found in Zr(TPP)$_2$ and could indicate slightly stronger π-π interactions. The electrochemical oxidation of Zr(OEP)$_2$ and Zr(TPP)$_2$ leads to mono and dications, which show near IR absorption bands at ~2000cm^{-1} higher energy than those of the corresponding cerium double-decker cations. The cations $[Zr(OEP)_2]X$, $[Zr(OEP)_2]X_2$ and $[Zr(TPP)_2]X$ (X = ClO_4^-, PF_6^-) can be isolated and were characterised by IR and NMR spectroscopy. The strong coupling of electron spins in the diamagnetic solid $[Zr(OEP)_2][ClO_4]_2$ were confirmed by magnetic susceptibility measurements (2K < T < 300K) [87].

Deprotonation of tmtaaH_2 (dibenzotetramethyltetraaza[14]annulene) by RLi (R = Me, ^{n}Bu) gives a red solid which can be crystallised as its DME derivative $[(tmtaa)_2Li_4(DME)_3]$. The reaction

of the lithium derivative in thf with $ZrCl_4(thf)_2$ gives [(tmtaa)$ZrCl_2$].2thf, in which the *cis*-$ZrCl_2$ moiety is located in the cavity of the saddle-shaped ligand. The reaction of $ZrCl_4(thf)_2$ with two equivalents of [(tmtaa)Li_2] or of [(tmtaa)$ZrCl_2$] with [(tmtaa)Li_2] gives the sandwich complex [(tmtaa)$_2$Zr], in which the metal achieves a cubic-type octacoordination (Figure 21). Both [(tmtaa)$ZrCl_2$] and [(tmtaa)$_2$Zr] have been the subject of single crystal X-ray diffraction studies. The former is diamagnetic and signals for the CH and CH_3 protons appear in the ^1H NMR spectra as a pair of singlets in CD_2Cl_2 and one singlet for both CH and CH_3 in CD_3CN. These are thought to result from the presence of two forms, depending on the saddle-shape conformation of the ligand in solution [88].

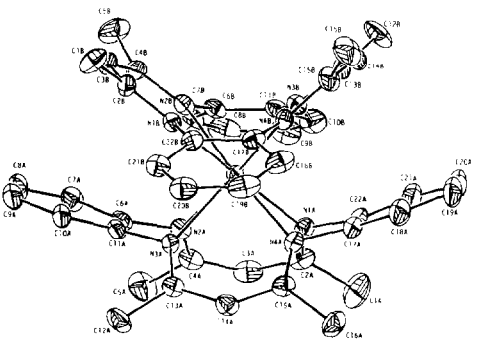

Figure 21. ORTEP drawing for the complex [(tmtaa)$_2$Zr] (30% probability ellipsoids). Reproduced with permission from ref. [88].

2.3.2 *Complexes with phosphorus donor ligands*

The reaction of $Cp^*_2ZrCl_2$ with two equivalents of $Li(thf)_2P(SiMe_3)_2$ in toluene yields $Cp^*_2Zr\{P(SiMe_3)_2\}_2$ in 81% yield. The presence of equivalent P atoms was indicated in solution by $^{31}P\{^1H\}$ NMR spectroscopic studies at 25 to 100°C. This fact was borne out by the solid state structure which shows two very similar Zr-P bonds (Zr-P1 2.634(2)Å, Zr-P2 2.600(2)Å) with each phosphido group having a near trigonal planar environment [89].

2.4 *ZIRCONIUM(0)*

Solutions of $(Me_3P)Zr(CO)_4$ readily undergo phosphine displacement in an excess of macrocyclic triamines such as 1,4,7-trimethyl-1,4,7-triazacyclononane (Me_3tacn) (equ (16)). All these complexes are air-sensitive and thermally stable, red to dark red microcrystalline materials. IR spectra of the tacn products have low frequency CO absorptions comparable to $[(C_5Me_5)M(CO)_4]^-$ species, whereas the Me_3tacn products have higher frequency CO absorptions similar to $[CpM(CO)_4]^-$ anions, indicating that tacn is the stronger neutral electron donor [90].

$$[(Me_3P)M(CO)_4] + L \xrightarrow[dme]{-25°C} [LM(CO)_4] + PMe_3$$

M =Zr, L = tacn, Me_3tacn
M = Hf, L = tacn

(16)

2.5 CATALYTIC USES OF ZIRCONIUM COMPLEXES

A chain transfer mechanism *via* β-CH_3 elimination has been proposed as the preferred mechanism for the polymerisation of propene by bis(pentamethylcyclopentadienyl) zirconium and hafnium dichloride/methylalumoxane catalysts at 50°C. The resulting atactic propene oligomers and low polymers have been shown by GC-MS and ^1H, ^{13}C NMR spectroscopic analysis to be mainly allyl and isobutyl terminated. The allyl/vinylidene ratio is 92/8 for Zr and 98/2 for Hf. In contrast the polymerisation of 1-butene occurs *via* exclusive β-H elimination and transfer to aluminum as with the non-substituted metallocenes Cp_2MCl_2 (M = Zr, Hf) [91].

Solid-state CPMAS ^{13}C NMR spectroscopy has been used to detect the formation and olefinic insertion reactivity of methylalumoxane-stabilised "cation-like" zirconocene alkyls. Various Al:Zr ratios of methylalumoxane:$Cp_2Zr(^{13}CH_3)_2$ were used and indicate that complete conversion to $[Cp_2Zr^{13}CH_3]^+$ occurs at lower Al:Zr ratios than those typically employed in catalytic reactions [92].

Catalysts derived from the reaction of $Cp^*_2ZrMe_2$ with $B(C_6F_5)_3$ or $B(C_6F_5)_4$ are active for the polymerisation of the functionalised diene and α-alkenes, 4-trimethylsiloxy-1,6-heptadiene, 5-tert-butyldimethylsiloxy-1-pentene and 5-(N,N-diisopropylamino)-1-pentene. The chiral (ethylene-1,2-bis(η5-4,5,6,7-tetrahydro-1-indenyl) catalysts, $[(EBTHI)ZrMe]^+X^-$, are more readily poisoned by silyl ethers compared to $[Cp^*_2ZrMe]^+X^-$ and generally give polymers whose spectroscopic data are consistent with highly isotactic microstructures [93].

Reactions of $CpCp^*M(SiR_3)Cl$ with hydrosilanes have been investigated (where M = Hf, Zr; R = Me, $SiMe_3$). In some cases the initial σ-bonded metathesis products react further *via* dihydro coupling e.g. $Cp_2Zr(SiMe_3)Cl$ reacts with $PhSiH_3$ to give Me_3SiH and $Cp_2Zr(SiH_2Ph)Cl$, which subsequently reacts with $PhSiH_3$ to give $[Cp_2ZrHCl]_n$, $PhH_2Si\text{-}SiH_2Ph$ and $PhH_2Si\text{-}SiHPh\text{-}SiH_2Ph$. For reasons that are not fully understood, the mixed ring $CpCp^*M(SiR_3)$ complexes participate in cleaner reactions. The σ-bond metathesis reactions are kinetically well-behaved in the dark but are photon-accelerated possibly *via* Zr-Si bond rupture. Reactions of d° Zr-Si bonds with alkoxysilanes were also examined. These redistribution reactions are catalysed by Cp^*ZrCl_3 and Cp'_2ZrX_2 (Cp' = Cp, Cp^*; X = H, alkyl, silyl, alkoxide, halide) (equ (17)) [94].

$$3\ HSiMe(OMe)_2 \xrightarrow[\text{or } CpCp^*Zr(OMe)_2]{[CpCp^*ZrH_2]_2} MeSiH_3 + 2\ MeSi(OMe)_3 \qquad (17)$$

Dehydrogenative polymerisation by Cp_2ZrMe_2 of pentamethyldisilane afforded a mixture of the oligosilanes, $Me_3Si[Me_2Si]_nSiMe_2H$, and with 1,1,2,2-tetramethyldisilane afforded $Me_2HSi[Me_2Si]_nSiHMe_2$ (n = 3-9) and with 1,2-dimethyldisilane afforded a unique cross-linked polysilane polymer $H[MeSiH]_nH$, (n = 3-14) [95]. The same dimethylzirconocene complex has been used in the dehydrogenative copolymerisation of $MeH_2Si_2H_2Me$ with itself and with $PhSiH_3$. The newly formed polymers $H[(MeSiH)_x(PhSiH)_y]_nH$ and $H[(MeSi)_x(Me_2Si)_y]_nH$ have been examined by gas liquid chromatography (glc) and glc-mass spectrometry [96].

The condensation of $RSiH_3$ (R = Ph, ^{n}Bu, ^{n}Hex) to silicon oligomers in the presence of the catalyst precursor Cp_2ZrCl_2 / 2 ^{n}BuLi has been monitored by gas chromatography, and the intermediate oligomers have been characterised by G.C. mass-spectrometry. In the case of the alkylsilanes, linear oligomers are produced initially but subsequently cyclic polysilanes are formed with increasing numbers of isomers as the number of silicon atoms increases [97].

A combination of *ab initio* electronic structure techniques and empirical force field molecular mechanices have been used to computationally reproduce the observed isotacticity for the *rac*-(1,2-ethylenebis(η^5-indenyl))zirconium and *rac*-(1,2-ethylenebis(η^5-tetrahydroindenyl))zirconium based Ziegler-Natta propylene polymerisation catalysts. Modifications to these catalysts to improve isotacticity have been proposed and the reduced reaction rate and atacticity for the corresponding *meso*-catalyst *meso*-(1,2-ethylenebis(η^5-indenyl))zirconium dichloride was calculated. A new syndiotactic catalyst is suggested in C_2H_4[cyclopentadienyl-1-(6,7,8,9,10,11,12,13-octahydrofluorenyl)]$ZrCl_2$ [98].

The catalyst system *rac*-ethylene(bis-indenyl) zirconium dichloride-methyl aluminoxane and its hafnium analogue have been used for the homopolymerisation of ethene and the copolymerisation of ethene and 1-butene. The zirconium system shows lower activities [99].

Efficient and selective zirconium-catalysed carbomagnesation with higher alkylmagnesium halides than EtMgCl has been achieved. In reactions of endo-5-norbornen-2-ol, five equivalents of n-alkylMgCl and 10 mol% Cp_2ZrCl_2, two secondary carbon stereogenic centres are formed with excellent levels of stereocontrol. A general mechanism for the carbomagnesation of bicyclic substrates has been proposed. An excess of alkylmagnesium halide is required for appreciable levels of selectivity and efficiency. The influence of Grignard reagents stems from the generation of the zirconacyclopentane (Figure 22) or the carbozirconate (Figure 23) complex.

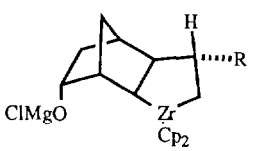

Figure 22

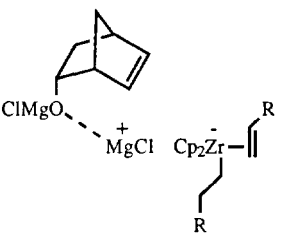

Figure 23

Deuterium labelling experiments indicate that an internal basic heteroatom controls the mode of cleavage of the intermediate five membered zirconacycle. It appears that the heteroatom binds and delivers magnesium to initiate a highly regioselective metallacyclopentane cleavage effecting Mg-Zr exchange with inversion of configuration [100].

Alternative reaction modes for α–alkene insertion into $[Cp_2Zr(CH_2{=}CH_2)CH_3]^+$ have been investigated by the extended Huckel M.O. Method. Agostic interaction of one of the α–H atoms of the migrating alkyl group with the Zr centre is found to stabilise the transition state of the preferred reaction mode (Figure 24) [101].

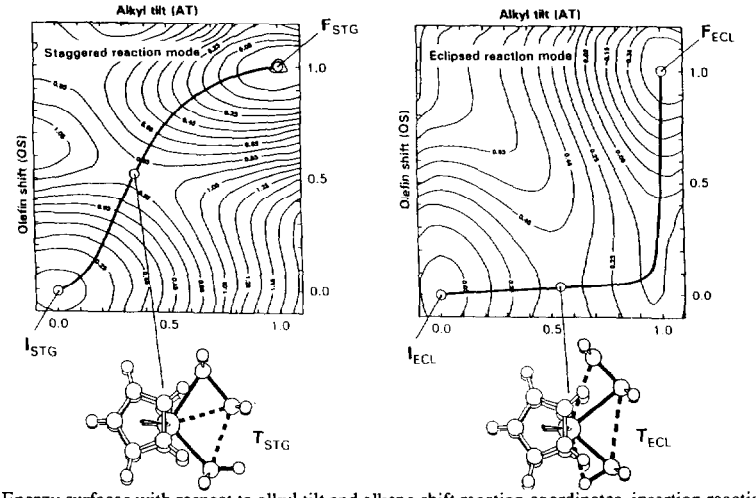

Figure 24. Energy surfaces with respect to alkyl tilt and alkene shift reaction coordinates, insertion reaction paths, and transition-state geometries for the staggered and eclipsed reaction modes. Reproduced from ref. [101] with permission.

Anions of the type $[(C_2B_9H_{11})_2M]^-$ (M = Fe, Co, Ni) are suitable non-coordinating anions for $[Cp_2ZrMe]^+$. Catalysts generated from Cp_2ZrMe_2 and $[PhMe_2NH][(C_2B_9H_{11})_2M]$ are active for the polymerisation and copolymerisation of ethene and α-alkenes in toluene or hexane. When M = Co, an exchange between the cation-anion pair and free amine takes place. When a 1:1 reaction mixture is observed using ^{13}C NMR spectroscopy spectroscopy at 25°C free $PhMe_2N$ is observed but as the temperature decreases (–40°C) new signals due to a new amine-coordinated species appear (equ (18)). This temperature dependent equilibrium has been followed by ^1H and ^{11}B NMR spectroscopy [102].

$$[Cp_2ZrMe][(C_2B_9H_{11})_2Co] + PhMe_2N \rightleftharpoons [Cp_2ZrMePhMe_2N][(C_2B_9H_{11})_2Co] \quad (18)$$

The $Cp_2MCl_2/^nBuLi$ (M = Zr, Hf) catalysed reactions of $PhMeSiH_2$ in the presence of near-stoichiometric quantities of cyclic and acyclic alkenes demonstrate a range of reactions dependent on the metal and the alkene. Hydrosilation of terminal acyclic alkenes and isomerisation/hydrosilation of internal alkenes occur with M = Zr when additional functional groups are present on the silicon: further elaboration can occur at the silicon atom or the silyl substituent is removed. Cyclic alkenes promote the formation of silicon oligomers, and dehydrocoupling of the vinyl hydrogen in cyclooctene and the hydrosilane occurs when M = Zr or Hf (equ (19)). It is proposed that these variations occur through the species $Cp_2M(H)SiPhMeH$ (M = Hf, Zr) *via* a σ-bond metathesis of either a hydrosilane or a cyclic alkene, or insertion into the MH or MSi bonds which eventually results in hydrosilyation or HC/SiH coupling [103].

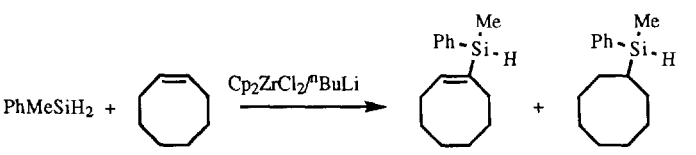

(19)

The complex $[ZrCp_2(CF_3SO_3)_2thf]$ is readily prepared from the reaction of zirconocene dichloride and $AgCF_3SO_3$ and is an efficient catalyst for the Diels-Alder reaction. Even at low catalyst loadings, rate accelerations of between 10^3 and $>10^5$ over the corresponding thermal reactions were observed. It is not universally applicable as it also acts as a slow polymerisation catalyst for 1,3-dienes e.g. in the reaction with either 1-cyclopentenone or methylacrylate the polymerisation side reaction dominates [104].

A series of $(\eta^5\text{–}5,6\text{-}X_2C_9H_5)_2ZrCl_2$ complexes (X = H, CH_3, OCH_3, Cl) were studied and found to be polymerisation catalysts, their catalytic activity decreasing with the presence of electron withdrawing substituents. A similar series of the racemic ethylene-bridged analogues (X = H, CH_3, OCH_3) were examined as polymerisation catalysts of propylene and ethylene. In these cases lower molecular weight polyethylene was produced. Notably the stereoselectivity of propylene insertion was sensitive to electronic effects with an increase in electron density at the metal centre leading to a decrease in the stereoselectivity. It is thought this may depend on the degree of α–agostic assistance during alkene insertion and/or the influence of the aluminoxane couterion [105].

The new cationic species $[(C_5H_4SiMe_3)_2ZrMe]^+$ and $[(C_5H_4SiMe_3)_2ZrMe(PhNEt_2)]^+$, prepared as in the scheme (Scheme 30) were examined for their ethene polymerisation activity. The latter was found to be comparable to that of the Cp_2ZrCl_2/methylaluminoxane system [106].

$$Cp'_2ZrMe_2 + [CPh_3]^+[BR_4]^- \longrightarrow [Cp'_2ZrMe]^+[BR_4]^- + Ph_3CMe$$
$$R = C_6H_3(CF_3)_2,\ C_6F_5$$

$$Cp'_2ZrMe_2 + [PhNHEt_2]^+[BR_4]^- \longrightarrow [Cp'_2ZrMe(PhNEt_2)]^+[BR_4]^- + CH_4$$
$$R = C_6F_5$$

Scheme 30

The hydrozirconation of 9-(Z)-octadecenylmethyl-sulfide, 9-(Z)-octadecenylphenyl sulfide and 9-(Z)-octadecenylphenyl sulphone was studied using three molar equivalents of $Cp_2Zr(H)Cl$. These compounds underwent substantial elimination of the functional group, yielding after hydrolysis large amounts of octadecane. As the saturated analogues, dodecylmethyl-sulfide, octadecylphenyl-sulfide and octadecenylphenyl sulfone, were unaffected by the hydrozirconation reagent, it was concluded that the C-S bonds are not cleaved by direct reaction [107].

When ZrO_2/SiO_2 catalysts are prepared by the sol-gel method (simultaneous gelation of zirconium acetate and tetraethoxysilane) in the presence of an acidic medium, the catalysts show high acidity and high specific surface area, between 27 and 805 $m^2\ g^{-1}$ [108].

Treatment of a series of *trans*-zirconacyclopentane complexes, generated from Cp_2ZrBu_2 and 1-butene, 1,6-heptadiene, 1,7-octadiene or dimethyldiallylsilane, with methanol followed by bromine or iodine, gave monohalogenated products with high stereoselectivity in good yield. From ^1H and ^{13}C NMR spectra it appears that the key reaction of these monohalogenations is the selective monoprotonation of the zirconacyclopentane complexes to give alkylalkoxyzirconocenes [109].

Zirconocene-alkene species react with alkenes to give zirconacyclopentanes and after hydrolysis the substituted alkane. In these reactions alkyl groups on the alkenes are located on the

β–position of the zirconacyclopentanes with 99% regioselectivity, whereas aryl groups are located on the α–position. Interestingly, the reaction of these zirconocene-alkenes with aldehydes gave the coupling products with the oppopsite orientation. Furthermore treatment of $(C_5Me_5)_2ZrEt_2$ with styrene gave 2-phenylbutane after hydrolysis, in contrast to the analogous reaction using Cp_2ZrEt_2 which gave 1-phenylbutane [110].

Tetra*kis*(neopentyl)zirconium reacts with a dehydroxylated silica surface (773K) to give $\equiv$Si-O-ZrNp$_3$. Under H_2 (423K, 400 torr) this complex is transformed into surface zirconium hydrides and silicon hydrides. The former activates the C-H bonds of cyclooctane and methane *via* a σ-bond metathesis reaction and selectively at low temperatures, hydrogenolyses alkanes such as neopentane, isobutane and propane. The proposed mechanism involves the activation of alkane C-H bonds and the C-C bond of the alkyl groups *via* a series of β–H migrations [111].

The catalytic activity of reduced CrO_x/ZrO_2 catalysts for propene hydrogenation was investigated at 195K in a flow apparatus. IR, ESR and catalytic results imply that the active sites for the hydrogenation are surface mononuclear Cr(III) species with three coordinate vacancies [112].

The effect of varying R on the catalytic behaviour of $(CpR)_2ZrCl_2$/ethylaluminoxane (R = H, Me, Et, ^{i}Pr, ^{t}Bu, $SiMe_3$, CMe_2Ph) for ethylene polymerisation was studied. The activity data shows a dependence on the steric (cone angle) and electronic (Hammett function) factors, with the catalytic activity increasing with the size and electron donating ability of the R substituents [113].

$(PhCH_2)_4Zr$, $C_5H_5Zr(CH_2Ph)_3$ and $(C_5H_5)_2Zr(CH_2Ph)_2$ form surface compounds on dehydroxylated alumina (15% α– and 85% δ–Al_2O_3) which on hydrogenolysis yield zirconium hydride species. The catalytic activity of the supported systems was studied in the partial hydrogenation of acetylene. The activity and selectivity of the $C_5H_5Zr(CH_2Ph)_3/Al_2O_3$ system was comparable to industrial Pd/Al_2O_3 catalysts [114].

The catalytic cyclometallation of styrene, m-methyl and p-tert-butylstyrene and 1-hexene with di-n-alkylmagnesiums (^nR_2Mg; R = Pr, Bu, hexyl) in the presence of Cp_2ZrCl_2 gave 2,4-disubstituted magnesacyclopentanes in high yield [115]. The regio- and stereo-selective synthesis of *trans*-3,4-dialkyl substituted aluminacyclopentanes has been acheived in the presence of (η^5–$C_5H_5)_2ZrCl_2$ [116]. Zirconium benzyl cyclopentadienyl compounds activated by $B(C_6F_5)_3$ were good catalysts for the homopolymerisation of ethene and propene on the addition of $AlMe_3$ [117].

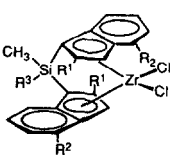

Figure 25.
R^1 = H, R^2 = H, R^3 = CH_3, H
R^1 = CH_3, R^2 = H, $^iC_3H_7$, R^3 = CH_3, C_6H_5
R^1 = C_2H_5, R^2 = H, R^3 = CH_3

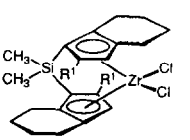

Figure 26.
R^1 = H, CH_3

Reproduced with permission from ref. [118].

The production of zirconium complexes (Figures 25 and 26) that successfully catalyse the synthesis of polypropylene of molecular mass > 100,000gmol^{-1} has been achieved. The most effective system, with $R^1 = CH_3$, $R^2 = {}^iC_3H_7$, $R^3 = CH_3$, gives polymers of molecular weight $460x10^3$ gmol^{-1} and provides distinctly improved isotacticity (98%). An X-ray crystal structure analysis of two of these related *ansa*-zirconocene compounds (R^1 = H, R^2 = H, $R^3 = CH_3$ and $R^1 = CH_3$, R^2 = H, $R^3 = CH_3$) shows that the difference in their catalytic activity is probably a result of electronic rather than steric factors with a decrease in the local Lewis acidity at the cationic zirconium atom of the active species, lowering its tendency to abstract a β–H atom, and thereby decreasing the number of chain terminations and increasing the molecular mass of the polymer [118].

A variety of linear and cyclic mono and dialkenes and aromatic substrates have been investigated for catalytic hydrogenation and isomerisation with $[Cp_2ZrH(CH_2PPh_2)]_n$. Selective formation of cycloheptene, cyclooctene and 1,2,3,4-tetrahydroanthracene is achieved using cycloheptatriene, cyclooctadiene (1,5 or 1,3-COD) and anthracene respectively. Catalytic isomerisation of 1-hexene to E-2-hexene and 1,5-COD to 1,3-COD occurs rapidly at 80°C. A kinetic study of the catalytic selective hydrogenation of 1,3-COD to cyclooctene was undertaken and gave some indication of the generation of an active homodimetallic Zr(IV)Zr(II) species in which both zirconium atoms are bridged by the diphenylphosphinomethyl ligand [119].

Ethene and propene homopolymerisation has been investigated by means of C_s-symmetry [2,4-cyclopentadien-1-ylidene(isopropylidene)fluoren-9-ylidene]zirconium dichloride/methyl aluminoxane and C_2-symmetry [(dimethylsilylene)bis(η^5–inden-1-ylidene)]zirconium dichloride/methyl aluminoxane catalyst systems in PhMe. The kinetic data show that the two catalysts behave differently concerning the stereospecifity and molecular weights of the polymers. This is thought to be a result of the differences in the symmetry and the angle between the planes of the π-ligand systems in the two catalysts [120].

Theoretical studies on the catalytic alkene polymerisation by silyene-bridged zirconocene complexes have been caried out, using an *ab initio* molecular orbital method. The transition state with approximate C_s-symmetry has a low activation barrier (~6.0 kcal mol^{-1}) compared to the π-complex formed from the primary insertion of ethene into $[(SiH_2Cp_2)ZrCH_3]^+$. Molecular mechanics (MM) calculations based on this type of transition state have shown that the substituents on the Cp rings of $[SiH_2(CpMe_n)_2ZrR]^+$ determine the conformation of the polymer chain end, and in turn, that the conformation of the fixed polymer chain end determines the stereochemistry of alkene insertion at the transition state. The same direct control mechanism is operational in the syndiotactic polymerisation of propene and 4-methyl-1-pentene [121].

ω-Hydroxyesters can be converted to the corresponding lactones over hydrated zirconium (IV) oxide in good yield. In particular heptanolide and octanolide are efficiently produced [122].

Proton NMR spectroscopy is used to study the monoalkylation by Al_2Me_6 of Cp_2ZrCl_2 interacting with methylaluminoxane. $AlMe_3$ contained in the methylaluminoxane seems to be the active species. It is postulated that Cp_2ZrCl_2 forms highly polarised species with an excess of methylaluminoxane, which decompose in the presence of a complexing agent such as KCl [123].

2.6 ZIRCONIUM INTERCALATION COMPOUNDS

Solid-state deuterium NMR spectroscopic investigations of an oriented film of a microcrystalliine ferrocenylethylamine zirconium hydrogen phosphate intercalation compound show that the ferrocenyl group lies with its C_5 axis parallel to the layers of the host solid [124].

Films of artifically controlled multilayers of zirconium and hafnium phosphonates have been prepared on a silicon substrate by immersing a silicon wafer modified with [$OHSiMe_2$-$(CH_2)_3$-PO_3H_2] as an anchoring agent, into aqueous solutions of $ZrOCl_2$, $H_2O_3P(CH_2)_{10}PO_3H_2$(DBPA), $HfOCl_2$, and DBPA [125].

The first solid-state ^{13}C and ^{31}P NMR spectroscopic study of uniaxially oriented films of zirconium bis(phosphonoacetic acid) has been undertaken to resolve the structure of the organic moiety. It is thought that solid-state packing-induced changes in the pendant organic group affect the ability of such species to interact with guest molecules. In $Zr(O_3PCH_2{}^{13}CO_2H)_2$ the P-C bond was found to lie perpendicular to the inorganic $Zr(O_3$-P-$)_2$ layers, while the P-C-C-O dihedral angle was calculated to be 75° to 90° [126].

A (s)-(+)-*N*-(3,5-dinitrobenzoyl)-L- leucine derivative was used as a chiral selector by intercalation into microcrystalline α-$Zr(HPO_4)_2.H_2O$. The enantioselectivity of the selector was unaffected by this intercalation and it successfully resulted in solutions in which the *ee* exceeded 90% [127].

The uptake of cden, [6-(2-aminoethylamino)-6-deoxy]-β-cyclodextrin, by γ-$Zr(HPO_4)_2.2H_2O$ has been studied at 25°C. The γ-phosphate initially forms an intercalated phase in which the cden molecules are arranged as a bilayer of thicknes 31.3Å; increasing amounts of cden decrease the intecalant layer to 24.7Å with an appreciable decrease in the cden content [128].

The electric conductivity of the following solid electrolytes with a β–$Fe_2(SO_4)_3$-type structure, $LiZr_2(PO_4)_3$, $MgZr_4(PO_4)_6$ and $ZnZr_4(PO_4)_6$ was enhanced by substitution of Si^{4+} for P^{5+}. The conductivity increased on increasing the concentration of the Li^+ in the lithium compound, or on increasing the compactness of the sintered specimen in the Mg and Zn compounds [129].

The effect on the composition of the Zr(IV) ions in $Zr(SO_4)_2.4H_2O$ (0.02-2.2 $molL^{-1}$ solutions) of the addition of alkali metal, alkaline earth metal and ammonium halides was studied. In the solid phases individual complexes were observed, the composition of which depended on the concentration of the metal in solution [130].

The mode of thermal decomposition of $Ti_xZr_{1-x}(HPO_4)_2.H_2O$ (x = 0.1, 0.2, 0.3, 0.45) was found to be similar to those of crystalline phosphates containing only Zr or Ti [131].

A variety of strategies have been employed to exchange intercalated Cu(II), Ni(II) and Zn(II) with protons or sodium ions and hence to regenerate the host α–zirconium phosphate. Strong acid (0.5M HCl) does affect deintercalation, but yields poorly crystalline α–ZrP. In the case of Cu(II) the introduction of acetylacetonate successfully yields crystalline α–ZrP. Deintercalation is thought to be favourable in this case due to the high formation constant of the $Cu(acac)_2$ complex. When ferrocenium or cobaltocenium-intercalated zirconium phosphates are reacted with 1% Na/Hg amalgam, deintercalation of 96-100% or 15-25% respectively was affected [132].

Two novel zirconium phosphonates with α–layered structures are reported, $Zr(O_3P(CH_2)_3NH_3^+)_2(Cl^-)_2$ with an interlayer spacing of 15.3Å and $Zr(O_3P(CH_2)_3NH_2)_{0.2}(O_3PCH_3)_{1.8}.2H_2O$ with an interlayer spacing of 10.4Å. The latter has a relatively porous interlayer gallery which allows protonation of the amine and inclusion and subsequent anion exchange; it also reacts with Cu(II) to give intercalation compounds [133].

2.7 *ZIRCONIUM CLUSTERS.*

Recent reports indicate that $[M_8C_{12}]^+$ (M = Zr, Hf) ions are the predominant products from the reactions of gaseous metal ions and clusters with gaseous hydrocarbons. Local density functional calculations yield two possible geometrical isomers (Th) for the $[Ti_8Cl_{12}]^+$ analogue [134, 135].

The preparation, crystal structure analyses and $^{31}P\{^1H\}$ NMR spectra of a series of ten electron empty octahedral hexazirconium clusters of general formula $[Zr_6X_{14}(PR_3)_4]$ have been obtained (X = Cl, R = Me, Pr, Et; X = Br, R = Me) (Figure 27). The syntheses involved reduction of ZrX_4 (X = Cl, Br) with two equivalents of $(^nC_4H_9)_3SnH$ in benzene or dichloromethane for 36 hours. One equivalent of phosphane was added to the resulting precipitate, giving a deep red solution of the products. The solid-state structures of these compounds show two distinct sets of Zr-Zr bond lengths (eq-eq, ax-ax) which result from a small tetragonal distortion of the metal frame (Zr bond lengths range from 3.167-3.450Å). Molecular orbital calculations were carried out by the SCF-Xα-SW method for the related C_{4v} symmetric clusters $[Zr_6Cl_{14}(PH_3)_4]$, $[Zr_6Cl_{14}(PH_3)_4H]$ and $[Zr_6Cl_{12}(PH_3)_6]$. The resulting electronic structures show that $[Zr_6Cl_{14}(PH_3)_4]$ should be strongly paramagnetic and that paramagnetism for $[Zr_6Cl_{14}(PH_3)_4H]$ is unavoidable due to its central hydrogen atom. Interestingly, the $^{31}P\{^1H\}$ NMR spectrum of a solution of $[Zr_6Cl_{14}(PEt_3)_4].2CH_2Cl_2$ shows some temperature dependent paramagnetism. The fact that this could be a result of a hydridic proton was excluded on these electronic grounds [136].

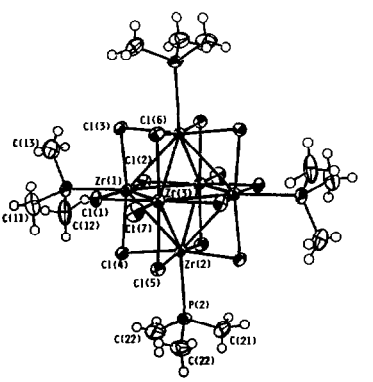

Figure 27. $[Zr_6Cl_{14}(PMe_3)_4]$ viewed along the Zr_{ax}-Cl_t bond. Hydrogen atoms have been given arbitrary thermal parameters and heavy atoms are represented by their ellipsoids at the 50% probability level. Reproduced with permission from ref. [136].

Octahedral metal clusters of the type $[Zr_6Cl_{12}Z]Cl_{6n}^-$ (n = 2-6, Z = Be, B, Fe) have been examined and features of their electronic spectra have been assigned using extended Hückel MO calculations to provide orbital energy orderings. The near IR diffuse reflectance spectra and solution spectra (acetonitrile) were similar and seemed to confirm the presence of the $(Zr_6Z)Cl_{12n-1}$ cluster core in solution. The energies for the dipole allowed transitions from the extended Huckel calculations gave satisfactory agreement with the observed values and the low-energy dipole allowed transitions were assigned as originating from a $^1t_{1u}$ (transition metal centred cluster) or a $^1t_{2g}$ (main group centred cluster) HOMO [137].

Two centered zirconium clusters were isolated from the reaction of Zr and $ZrCl_4$ with RbCl plus graphite, or LiCl plus $ZrH_{1.7}$ at ~850 or 700°C respectively. The structures of these two compounds were established by single crystal X-ray diffraction. $Rb_4Zr_6Cl_{18}C$, consists of individual close-packed layers of isolated $[Zr_6(C)Cl^i_{12}Cl^a_6]^{4-}$ clusters. The rhombohedral $Li_6Zr_6Cl_{18}H$ contains cubic-close packed $\{[Zr_6(H)Cl^i_{12}]Cl^a_6\}^{6-}$ clusters with lithium in *pseudo*octahedral cavities between and within the layers [138].

REFERENCES

1. J.E. Gozum, S.R. Wilson and G.S. Girolami, *J. Am. Chem. Soc.*, 114 (1992) 9483.
2. Z-Y. Guo, P.K. Bradley and R.F. Jordan, *Organometallics*, 11 (1992) 2690.
3. J.E. Bercaw and J.R. Moss, *Organometallics*, 11 (1992) 639.
4. F. Mohamadi and M.M. Spees, *Organometallics*, 11 (1992) 1398.
5. A.L. Rheingold, N.P. Robinson, J. Whelan and B. Bosnich, *Organometallics*, 11 (1992) 1869.
6. B. Rieger, *J. Organomet. Chem.*, 428 (1992) C33.
7. A. Horton and A.G. Orpen, *Organometallics*, 11 (1992) 1193.
8. T. Cuenca, J.C. Flores, P. Royo, A-M. Larsonneur, R. Choukroun and F. Dahan, *Organometallics*, 11 (1992) 777.
9. A. Razavi and J. Ferrara, *J. Organomet. Chem.*, 435 (1992) 299.
10. A.D. Horton and A. G. Orpen, *Angew. Chem., Int. Ed., Engl.*, 31 (1992) 876.
11. K. Mashima and A. Nakamura, *J. Organomet. Chem.*, 428 (1992) 49.
12. M.E. Huttenloch, J. Diebold, U. Rief, H.R. Brintzinger, A.M. Gilbert and T.J. Katz, *Organometallics*, 11 (1992) 3600.
13. B. Rieger, M. Steimann and R. Fawzi, *Chem. Ber.*, 125 (1992) 2373.
14. K. Dey, D. Bandyopadhyay, K.K. Nandi, S.N. Poddar, G. Mukhopadhyay and G.B. Kauffman, *Synth. React. Inorg. Met. Org. Chem.*, 22 (1992) 1111; *Chem. Abstr.*, 118 (1992) 124703f.
15. A.D. Horton, *Organometallics*, 11 (1992) 3271.
16. A.D. Horton, *J. Chem. Soc., Chem. Commun.*, 2 (1992) 185.
17. I.E. Nifant'ev, A.V. Churakov, I.F. Urazowski, Sh.G. Mkoyan and L.O. Atovmyan, *J. Organomet. Chem.*, 435 (1992) 37.
18. E. Ciliberto, S. DiBella, A. Gulino, I. Fragala, J.L. Petersen and T.J. Marks,*Organometallics*, 11 (1992) 1727.
19. T.R. Cundari and M.S. Gordon *Organometallics*, 11 (1992) 3122.
20. P.J. Walsh, A.M. Baranger and R.G. Bergman, *J. Am. Chem. Soc.*, 114 (1992) 1708.
21. G. Erker, R. Pfaff, C. Kruger, M. Nolte and R. Goddard, *Chem. Ber.*, 125 (1992) 1669.
22. P.J. Walsh, F-J. Hollander and R.G. Bergman, *J. Organomet. Chem.*, 428 (1992) 13.
23. W.A. Herrmann, N.W. Huber and J. Behm, *Chem. Ber.*, 125 (1992) 1405.
24. Y. Bai, H.W. Roesky, M. Noltemeyer and M. Witt, *Chem. Ber.*, 125 (1992) 825.
25. N. Kuhn, S. Stubenrauch, R. Boese and D. Blaser, *J. Organomet. Chem.*, 440 (1992) 289.
26. M.M. Banaszak Hall and P.T. Wolczanski, *J. Am. Chem. Soc.*, 114 (1992) 3854.
27. T.R. Cundari, *J. Am. Chem. Soc.*, 114 (1992) 10557.
28. H. Brand and J. Arnold, *J. Am. Chem. Soc.*, 114 (1992) 2266.
29. J. Arnold, S.E. Johnson, C.B. Knobler and M.F. Hawthorne, *J. Am. Chem. Soc.*, 114 (1992) 3996.

30. F.R. Lemke, D.J. Szalda and R.M. Bullock, *Organometallics*, 11 (1992) 876.
31. D.F. Evans, G.W. Griffiths, C.O.'Mahoney, D.J. Williams, C.Y. Wong and J.D. Woollins, *J. Chem. Soc., Dalton Trans.*, 16 (1992) 2475.
32. R.L. Davidovich, V.B. Logvinova and L.V. Teplukhina, *Koord. Khim.*, 18 (1992) 580; *Chem. Abstr.*, 117 (1992) 203955x.
33. A.S. Guram, D.C. Swenson and R.F. Jordan, *J. Am. Chem. Soc.*, 114 (1992) 8991.
34. K. Plossl, J.R. Norton, J.G. Davidson and E. Kent Barefield, *Organometallics*, 11 (1992) 534.
35. Z. Hou and D.W. Stephan, *J. Am. Chem. Soc.*, 114 (1992) 10088.
36. H.H. Karsch, G. Grauvogl, B. Deubelly and G. Muller, *Organometallics*, 11 (1992) 4238.
37. H.H. Karsch, B. Deubelly, G. Grauvogl, J. Lachmann and G. Muller, *Organometallics*, 11 (1992) 4245.
38. N. Dufour, A-M. Caminiade, M. Basso-Bert, A. Igau and J-P. Majoral, *Organometallics*, 11 (1992) 1131.
39. G.M. Diamond, M.L.H. Green, N.M. Walker, J.A.K. Howard and S.A. Mason, *J. Chem. Soc., Dalton Trans.*, 17 (1992) 2641.
40. G.M. Diamond, M.L.H. Green, P. Mountford, N.M. Walker and J.A.K. Howard, *J. Chem. Soc., Dalton Trans.*, 3 (1992) 417.
41. E. Hey-Hawkins and F. Lindenberg, *Chem. Ber.*, 125 (1992) 1815.
42. K. Fromm, G. Baum and E. Hey-Hawkins, *Z. Anorg. Allg. Chem.*, 615 (1992) 35; *Chem. Abstr.*, 118 (1992) 7108e.
43. T.L. Breen and D.W. Stephan, *Inorg. Chem.*, 31 (1992) 4019.
44. P. Binger, F. Langhauser, B. Gabor, R. Mynott, A.T. Herrmann and C. Kruger, *J. Chem. Soc., Chem. Commun.*, 6 (1992) 505.
45. G. Erker, R. Petrenz, C. Kruger and M. Nolte, *J. Organomet. Chem.*, 431 (1992) 297.
46. G. Erker, R. Petrenz, C. Kruger, F. Lutz, A. Weiss and S. Werner, *Organometallics*, 11 (1992) 1646.
47. R. Beckhaus, D. Wilbrandt, S. Flatau and W-H. Bohmer, *J. Organomet. Chem.*, 423 (1992) 211.
48. H.G. Alt, C.E. Denner and R. Zenk, *J. Organomet. Chem.*, 433 (1992) 107.
49. B.H. Lipshutz and R. Keil, J. Am. Chem. Soc., 114 (1992) 2919.
50. H. Gornitzka, F.T. Edelmann and K. Jacob, *J. Organomet. Chem.*, 436 (1992) 325.
51. H-M. Gau, C-T. Chen and C-C. Schei, *J. Organomet. Chem.*, 424 (1992) 307.
52. U. Schubert, H. Buhler and B. Hirle, *Chem. Ber.*, 125 (1992) 999.
53. G. Erker, M. Rump, C. Kruger and M. Nolte, *Inorg. Chim. Acta*, 198-200 (1992) 679; *Chem. Abstr.*, 117 (1992) 234165u.
54. M.J. Carney, P.J. Walsh, F.J. Hollander and R.G. Bergman, *Organometallics*, 11 (1992) 761.
55. R. Broussier, A. Da Rold and B. Gautheron, *J. Organomet. Chem.*, 427 (1992) 231.
56. H-M. Gau, C-C. Schei, L-K. Lui and L-H. Luh, *J. Organomet. Chem.*, 435 (1992) 43.
57. I.M. Saidul and U.M. Masir, *Synth. React. Inorg. Met.-Org. Chem.*, 22 (1992) 893; *Chem. Abstr.*, 117 (1992) 203928r.
58. F. Quignard, C. Lecuyer, C. Bougault, F. Lefebvre, A. Choplin, D. Olivier and J-M. Basset, *Inorg. Chem.*, 31 (1992) 928.
59. G. Hall and H. Sutcliffe, *Thermochim. Acta*, 205 (1992) 323; *Chem. Abstr.*, 117 (1992) 199333y.
60. J. Cacciola, K.P. Reddy and J.L. Petersen,*Organometallics*, 11 (1992) 665.
61. W.E. Piers, L. Koch, D.S. Ridge, L.R. MacGillivray and M. Zaworotko, *Organometallics*, 11 (1992) 3148.
62. Z-Q. Wang, S-W. Lu, H-F. Guo and N-H. Hu, *Polyhedron*, 11 (1992) 39.
63. Z-Q. Wang, S-W. Lu, H-F. Guo and N-H. Hu, *Polyhedron*, 11 (1992) 1131.
64. L.K. Myers, C. Langhoff and M.E. Thompson, *J. Am. Chem. Soc.*, 114 (1992) 7560.
65. S.C. Sockwell, P.S. Tanner and T.P. Hanusa, *Organometallics*, 11 (1992) 2634.
66. Y.A. Andrianov and V.P. Maryin, *J. Organomet. Chem.*, 441 (1992) 419.
67. G. Erker, R. Noe, C. Kruger and S. Werner, *Organometallics*, 11 (1992) 4174.
68. G. Erker, M. Albrecht, C. Kruger, S. Werner, P. Binger and F. Langhauser, *Organometallics*, 11 (1992) 3517.
69. G. Erker, M. Albrecht, S Werner, M. Nolte and C. Kruger, *Chem. Ber.*, 125 (1992) 1953.
70. G. Erker, M. Albrecht, C. Kruger and S. Werner, *J. Am. Chem. Soc.*, 114 (1992) 8531.
71. J.A. Samuels, J.W. Zwanziger, E.B. Lobkovsky and K.G. Caulton, *Inorg. Chem.*, 31 (1992) 4046.
72. W.E. Piers, R.M. Whittal, G. Ferguson, J.F. Gallagher, R.D.J. Froese, H.J. Stronks and P.H. Krygsman, *Organometallics*, 11 (1992) 4015.

73. H-G. Woo, W.P. Freeman and T.D. Tilley, *Organometallics*, 11 (1992) 2198.
74. J. Bodiguel, P. Meunier, M.M. Kubicki, P. Richard and B. Gautheron, *Organometallics*, 11 (1992) 1423.
75. V. Christou and J. Arnold, *J. Am. Chem. Soc.*, 114 (1992) 6240.
76. T. Bartik, B. Happ, A. Sieker, S. Stein, A. Sorkau, K.H. Thiele, C. Kriebel and G. Palyi, *Z. Anorg. Allg. Chem.*, 608 (1992) 173; *Chem. Abstr.*, 117 (1992) 19151f.
77. F.R. Lemke and R.M. Bullock, *Organometallics*, 11 (1992) 4261.
78. Y. Raoult, R. Choukroun and C. Blandy, *Organometallics*, 11 (1992) 2443.
79. X. Yang, C.L. Stern and T.J. Marks, *Angew. Chem., Int. Ed., Engl.*, 31 (1992) 1375.
80. T. Cuenca, R. Gomez, P. Gomez-Sal, G.M. Rodriguez and P. Royo, *Organometallics*, 11 (1992) 1229.
81. D.J. Arney, M.A. Bruck, S.R. Huber and D.E. Wigley, *Inorg. Chem.*, 31 (1992) 3749.
82. D.M. Hoffman and S. Lee, *Inorg. Chem.*, 31 (1992) 2675.
83. J. Ho and D.W. Stephan, *Organometallics*, 11 (1992) 1014.
84. P.B. Hitchcock, M.F. Lappert, G.A. Lawless, H. Olivier and E.J. Ryan, *J. Chem. Soc., Chem. Commun.*, 6 (1992) 474.
85. K. Shibata, T. Aida and S. Inoue, *Chem. Lett.*, 7 (1992) 1173.
86. H-J. Kim, D. Whang, J. Kim and K. Kim, *Inorg. Chem.*, 31 (1992) 3882.
87. J.W. Buchler, A. De Cian, S. Elschner, J. Fischer, P. Hammerschmitt and R. Weis, *Chem. Ber.*, 125 (1992) 107.
88. S. deAngelis, E. Solari, E. Gallo, C. Floriani, A. Chiesi-Villa and C. Rizzoli, *Inorg. Chem.*, 31 (1992) 2520.
89. F. Lindenberg and E. Hey-Hawkins, *J. Organomet. Chem.*, 435 (1992) 291.
90. J.E. Ellis, A.J. DiMaio, A.L. Rheingold and B.S. Haggerty, *J. Am. Chem. Soc.*, 114 (1992) 10676.
91. L. Resconi, F. Piemontesi, G. Franciscono, L. Abis and T. Fiorari, *J. Am. Chem. Soc.*, 114 (1992) 1025.
92. C. Sishta, R.M. Hathorn and T.J. Marks, *J. Am. Chem. Soc.*, 114 (1992) 1112.
93. M.R. Kesti, G.W. Coates and R.M. Waymouth, *J. Am. Chem. Soc.*, 114 (1992) 9679.
94. H.G. Woo, R.H. Heyn and T.D. Tilley, *J. Am. Chem. Soc.*, 114 5698.
95. E. Hengge and M. Weinberger, *J. Organomet. Chem.*, 433 (1992) 21.
96. E. Hengge and M. Weinberger, *J. Organomet. Chem.*, 441 (1992) 397.
97. J.Y. Corey and X-H. Zhu, *J. Organomet. Chem.*, 439 (1992) 1.
98. L.A. Castanguay and A.K. Rappe, *J. Am. Chem. Soc.*, 114 (1992) 5832.
99. K. Heiland and W. Kaminsky, *Makromol. Chem.*, 193 (1992) 601; *Chem. Abstr.*, 118 (1992) 236229w.
100. A.H. Hoveyda, J.P. Morken, A.F. Houri and Z. Xu, *J. Am. Chem. Soc.*, 114 (1992) 6692.
101. M-H. Prosene, C. Janiak and H-H Brintzinger, *Organometallics*, 11 (1992) 4036.
102. G.G. Hlatky, R.R. Eckman and H.W. Turner, *Organometallics*, 11 (1992) 1413.
103. J. Corey and X-H. Zhu, *Organometallics*, 11 (1992) 672.
104. T.K. Hollis, N.P. Robinson and B. Bosnich, *Organometallics*, 11 (1992) 2745.
105. I-M. Lee, W.J. Gauthier, J.M. Ball, B. Iyenger and S. Collins, *Organometallics*, 11 (1992) 2115.
106. M. Bochmann and S.J. Lancaster, *J. Organomet. Chem.*, 434 (1992) C1.
107. S. Karlsson, A. Hallberg and S. Gronowitz, *J. Organomet. Chem.*, 430 (1992) 53.
108. T. Lopez, R. Gomez, G. Ferrat, J. M. Dominguez and I. Schifter, *Chem. Lett.*, 10 (1992) 1941.
109. T. Takahashi, K. Aoyagi, R. Hara and N. Suzuki, *Chem. Lett.*, 9 (1992) 1693.
110. T. Takahashi, N. Suzuki, M. Hasegawa, Y. Nitto, K-I. Aoyagi and M. Saburi, *Chem. Lett.*, 2 (1992) 331.
111. F. Quignard, C. Lecuyer, A. Choplin, D. Olivier and J.M. Basset, *J. Mol. Catal.*, 74 (1992) 353; *Chem. Abstr.*, 118 (1992) 6506w.
112. V. Indovina, A. Cimino, S. De Rossi, G. Ferraris, G. Ghiotti and A. Chiorino, *J. Mol. Catal.*, 75 (1992) 305; *Chem. Abstr.*, 118 (1992) 12242y.
113. P.C. Mohring and N.J. Coville, *J. Mol. Catal.*, 77 (1992) 41; *Chem. Abstr.*, 118 (1992) 22719y.
114. F. Rehbaum and K.H. Thiele, *J. Prakt. Chem./Chem.-Ztg.*, 334 (1992) 512; *Chem. Abstr.*, 118 (1992) 38429q.
115. U.M. Dzhemilev, R.M. Sultanov, R.G. Gaimaldinov, R.R. Muslukhov, S.I. Lomakina and G.A. Tolstikov, *Izu. Akad. Nauk. Ser. Khim.*, 4 (1992) 980; *Chem. Abstr.*, 118 (1992) 80973n.
116. U.M. Dzhemilev, A.G. Ibragimov and A.B. Morozov, *Mendeleev Commun.*, 1 (1992) 26.

117. C. Pellecchia, A. Proto, P. Longo and A. Zambelli, *Makromol. Chem. Rapid. Commun.*, 13 (1992) 277; *Chem. Abstr.*, 118 (1992) 256143s.
118. W. Spaleck, M. Antberg, J. Rohrmann, A. Winter, B. Bachmann, P. Kiprof, J. Behm and W.A. Herrmann, *Angew. Chem., Int. Ed., Engl.*, 31 (1992) 1347.
119. Y. Raoult, R. Choukroun, M. Basso-Bert and D. Gervais, *J. Mol. Catal.*, 72 (1992) 47; *Chem. Abstr.*, 117 (1992) 7230t.
120. N. Herfert and G. Fink, *Makromol. Chem.*, 193 (1992) 1359; *Chem. Abstr.*, 117 (1992) 151493y.
121. H. Kawamura-Kuribayashi, N. Koga and K. Morokuma, *J. Am. Chem. Soc.*, 114 (1992) 8687.
122. H. Kuno, M. Shibagaki, T. Takahashi, I. Honda and H. Matsushita, *Chem. Lett.*, 4 (1992) 571.
123. D. Cam and U. Giannini, *Makromol. Chem.*, 193 (1992) 1049; *Chem. Abstr.*, 117 (1992) 8565t.
124. C.F. Lee, L.K. Myers, K.G. Valentine and M.E. Thompson, *J. Chem. Soc., Chem. Commun.*, 2 (1992) 201.
125. Y. Umemura, K-I. Tanaka and A. Yamagishi, *J. Chem. Soc., Chem. Commun.*, 1 (1992) 67.
126. D.A. Burwell, K.G. Valentine, J.H. Timmermans and M.E. Thompson, *J. Am. Chem. Soc.*, 114 (1992) 4144.
127. G. Cao, M.E. Garcia, M. Alcala, L.F. Burgess and T.E. Mallouck, *J. Am. Chem. Soc.*, 114 (1992) 7574.
128. T. Kijima and K. Ohe, *J. Chem. Soc., Dalton Trans.*, 19 (1992) 2877.
129. K. Nomura, S. Ikeda, K. Ito and H. Einaga, *Chem. Lett.*, 10 (1992) 1897.
130. M.M. Godneva, D. L. Motov and R.F. Okhrimenko, *Zh. Noerg. Khim.*, 37 (1992) 1322; *Chem. Abstr.*, 118 (1992) 28019s.
131. S.K. Shakshooki, S.A. Khalil, A.S.M. Abuhamaira, L. Szirtes and Z. Poko, *J. Therm. Anal.*, 38 (1992) 1571; *Chem. Abstr.*, 118 (1992) 51299s.
132. G.L. Rosenthal and J. Caruso, *Inorg. Chem.*, 31 (1992) 144.
133. G.L. Rosenthal and J. Caruso, *Inorg. Chem.*, 31 (1992) 3104.
134. I. Dance, *J. Chem. Soc., Chem. Commun.*, 24 (1992) 1779.
135. R.W. Grimes and J.D. Gale, *J. Chem. Soc., Chem. Commun.*, 17 (1992) 1222.
136. F.A. Cotton, X. Feng, M. Shang and W.A. Wojtczak, *Angew. Chem., Int. Ed., Engl.*, 31 (1992) 1050.
137. M.R. Bond and T. Hughbanks, *Inorg. Chem.*, 31 (1992) 5015.
138. J. Zhang, R.P. Ziebarth and J.D. Corbett, *Inorg. Chem.*, 31 (1992) 614.